Isolation and Characterization of Anti-malarial Compounds

From a Natural Product Library

By

Holly Marie Carrell

Thesis

Submitted to the faculty of the

Graduate school of Vanderbilt University

In partial fulfillment of the requirements

For the degree of

MASTER OF SCIENCE

In

Chemistry

August, 2013

Nashville, Tennessee

Approved:

Professor David W. Wright

Professor Brian O. Bachmann

TABLE OF CONTENTS

Page

LIST OF TABLES

LIST OF FIGURES

Chapter I

Hemozoin: Crystal Engineering Survivability

(Chapter I taken from Hemozoin: Crystal Engineering Survivability, published in the

Encyclopedia of inorganic and Bioinorganic Chemistry, 2012)

Introduction

In nature, biomineralization is observed across the entire biosphere. These biologically

synthesized materials can consist of carbonate, phosphate, oxalate, silica, iron, go2ld

and many other diverse compositions of organic or inorganic materials. The most well-

known examples of biomineralization are those that lend structural support to a species,

including the formation of bones in vertebrates and the shells of eggs. Magnetotactic

bacteria also rely on the formation of magnetic nanometer-size Fe_3O_2 crystallites in

order to locate oxygen-rich environments by sensing the Earth's geomagnetic field. The

formation of these biominerals generally occurs under physiological conditions in a

highly controlled and organized sequence of events. Another biomineral, hemozoin, is a

heme crystal synthesized by the malaria parasite as a survival mechanism to escape

heme related toxicity. The discovery of this detoxification biomineral actually precedes

the discovery of the malaria parasite itself. Although hemozoin has been studied since

the 18th century, scientists have only begun to obtain a detailed understanding of the

structure and formation of this biomineral in the last twenty five years. Hemozoin

formation is an important drug target in antimalarial drug discovery and development. In fact, the most successful antimalarial developed to date, chloroquine, acts by disrupting formation of hemozoin. Unfortunately, chloroquine is now ineffective as an antimalarial due to the emergence 2of multidrug-resistant strains of the parasite, though hemozoin remains a viable drug target in antimalarial drug discovery. In order to develop new antimalarial compounds that target the formation of hemozoin, it is important to have a sound understanding of the formation of this biocrystal.

Homeostasis of Heme

The internal environment of all biological systems must be carefully regulated. The heme molecule is a perfect example of the importance of this homeostasis. Heme is essential to aerobic organisms, playing important roles in many biological reactions such as oxygen transport, respiration, drug detoxification and signal transduction (*1-4*). However, when heme is released in an uncontrolled fashion into a living organism it can become extremely toxic. One example demonstrating the toxic effects of heme is seen in rhabdomylosis. Here, trauma or injury results in the rapid breakdown of muscle tissue, releasing myoglobin into the bloodstream. This harmful heme-containing protein is not normally found in blood. In the kidney, heme exposure promotes oxidative stress in renal cells by increasing lipid peroxidation, and can cause local inflammatory reactions ultimately leading to renal failure (*5, 6*). The ability of heme to promote oxidative stress can be attributed to the presence of the redox-active iron center that can generate reactive oxygen species (ROS), leading to damage to lipids, proteins, and

DNA. Free heme has also been shown to interact with proteins, catalyzing the

degradation of proteins into small peptide fragments and causing covalent cross-linking

of Apolipoprotein B, triggering atherosclerosis (7). Studies have also shown that

exposure to heme results in nicking and degradation of DNA. The mtDNA of liver cells

shows that the large region that codes for cytochrome c oxidase and NADH

dehydrogenase is deleted in cells exposed to hemin. This mtDNA damage leads to the

altered expression of mitochondrial cell death proteins, suggesting a role of hemin in

influencing apoptosis (8).

Detoxification of Heme in Humans

As protection against the drastic toxic effects of free heme, humans are

equipped with several detoxification mechanisms. Primarily, heme detoxification is

carried out by the heme oxygenase (HO) systems (HO-1, HO-2 and HO-3), and by extra-

HO systems less frequently, including hemopexin and albumin (9). These HO enzymes

play a large role in protecting cells from the oxidative stress caused by free heme by

working with NADPH–cytochrome P450 to break down the porphyrin ring into

equimolar amounts of free iron, biliverdin, and carbon monoxide (10). In this process,

HO transfers reducing equivalents to the α-methene bridge of heme from NADPH-

cytochrome P-450 reductase to open the tetra-pyrrolic ring, freeing CO and biliverdin.

Biliverdin is then converted to bilirubin by biliverdin reductase, conjugated to glucuronic

acid, and excreted from the body (Figure 1) (11, 12). The HO systems are very efficient

at detoxifying free heme and restoring homeostasis in the organisms that have them,

but organisms that lack the HO systems have developed alternative mechanisms to

protect themselves from free heme toxicity.
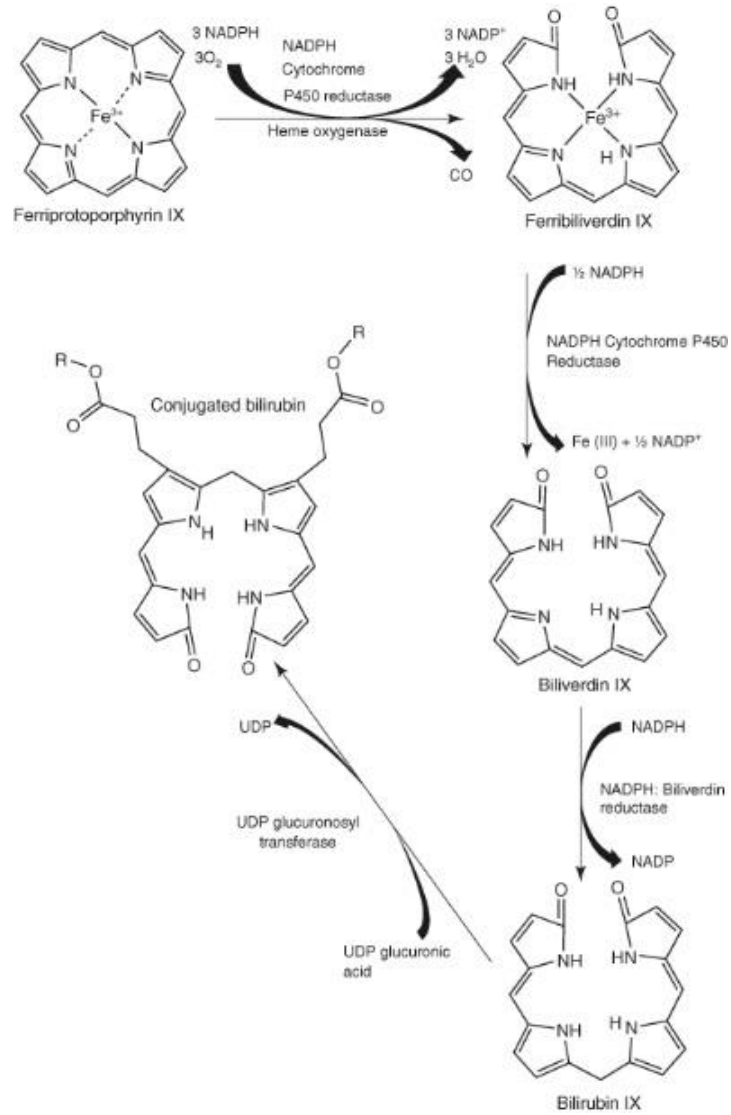
Figure 1. Pathway of free heme detoxification by Heme
Oxygenase.

<u>*Heme Detoxification in the Malaria Parasite*</u>

One organism lacking a HO system is the parasite responsible for malaria. Malaria is caused by several species of intracellular parasites of the *Plasmodium* genus. Of this genus, there have been at least 200 species identified, with *P. falciparum* being the primary causative agent of human malaria. The lifecycle of the malaria parasite is quite complex (Figure 2). *P. falciparum* sporozoites are transmitted to humans through the saliva of a female Anopheles mosquito during a blood meal. Once in the host's bloodstream, *P. falciparum* sporozites invade the hepatocytes and undergo a phase of growth and differentiation followed by the release of merozoites into the bloodstream. The merozoites then enter host red blood cells, referred to as the the intraerythrocytic stage of infection. This stage is characterized by the onset of the symptoms of a malaria infection. Inside the erythrocyte, the parasite goes through three distinct growth phases that can be distinguished under a light microscope. The ring stage is first, lasting about 24 hours. The second stage is the very active trophozoite stage. It is during this stage that most of the erythrocyte cytoplasm is consumed. Third , the parasite undergoes 4-5 cycles of binary divisions, producing merozoites that eventually rupture the red blood cell membrane, and enter the bloodstream to infect new red blood cells (13). During this intraerythrocytic cycle, the host cytoplasm is consumed, and an estimated 60-80% of available hemoglobin is degraded for use as a nutrient source (14). During this degradation process, the amino acids obtained from hemoglobin catabolism are incorporated into *P. falciparum* proteins and used for energy metabolism (15) (16-18).

The amino acids *P. falciparum* cannot obtain from hemoglobin are readily scavenged
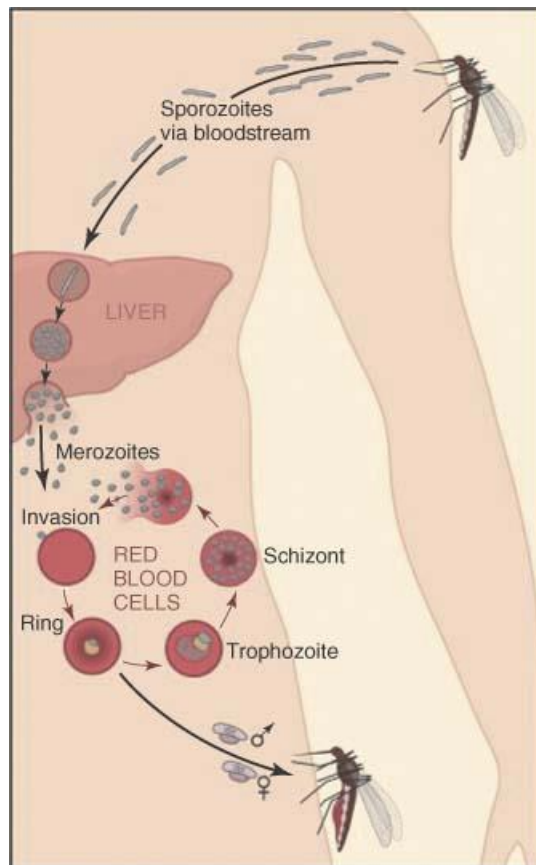
from the environment (19, 20).

Figure 2. Life-cycle of Plasmodium falciparum
in the human host.

The malaria parasite obtains hemoglobin from the cytosol through invagination

of the parasitophorous vacuolar and plasma membrane, creating a double membrane

vesicle. These vesicles fuse together, creating a single membrane digestive food vacuole.

Once formed, the digestive food vacuole becomes the primary site of hemoglobin

digestion (21, 22). This specialized organelle maintains an acidic environment, estimated

pH of 4.8 (19, 23). Inside this organelle, aspartic and cysteine protease activities have

been detected that are the primary enzymes responsible for globin proteolysis. Aspartic

proteases make up about 60-80% of enzyme activity, while cysteine proteases make up

20-40% (24, 25). The process of hemoglobin degradation has been found to occur in a

specific order, requiring an initial aspartic protease cleavage, followed by secondary

aspartic protease and cysteine protease cleavages (26). Vacuolar degradation produces

small polypeptides, but no free amino acids. This suggests that cleavage of the small

peptide fragments occurs in the cytoplasm, outside of the digestive vacuole (26-28).

Sequencing of the *P. falciparum* genome has found at least ten genes encoding

aspartic proteases, plasmepsins I, II, IV-X, and histo-aspartic protease (HAP) (26, 28).

HAP is 60% homologous to plasmepsins I and II, but has several substitutions, one of

which is the replacement of the catalytic aspartate with a histidine (29). Of the ten

genes that encode plasmepsins in *P. falciparum*, three are not expressed in

intraerythrocytic growth stages (plasmepsins VI, VII, and VIII), and three are expressed,

but do not seem to be active in the digestive food vacuole (plasmepsins V, IX, and X).

Plasmepsins I, II, IV, and HAP are the only aspartic proteases that are found in the

digestive food vacuole, and participate in hemoglobin degradation. Plasmepsin I has

been shown to cleave hemoglobin between α33Phe-34Leu with exceptional specificity

(30). This is significant because the α33-34 bond is in the hinge region of the hemoglobin

molecule. This region is responsible for holding the protein together when oxygen is

bound. Cleaving this domain unravels the heme molecule, exposing other amino acid residues for cleavage by the secondary proteases (31). Plasmepsins II and IV have been shown to cleave native hemoglobin, but prefer to cleave already denatured hemoglobin indicating that they function primarily as secondary proteases (28, 32, 33). HAP is a secondary protease, showing less efficiency in cleaving the α33-34 bond of native hemoglobin, although it is a full order of magnitude faster than the other plasmepsins at cleaving denatured globin at other sites (28, 32, 34).

The *P. falciparum* genome encodes four falcipains; falcipain I, II, II' and falcipain III (28, 33, 35). Falcipain I has not been shown to be involved in hemoglobin degradation, but falcipains II and III have acidic optimal pH, and are localized in the digestive food vacuole, indicating their involvement in hemoglobin digestion (33). Both falcipain II and III are capable of hydrolyzing native and denatured hemoglobin, but falcipain II has been shown to be more active against peptidyl substrates compared to falcipain III (36-38).

Finally, a metalloprotease, falcilysin, also participates in the hemoglobin degradation pathway. Falcilysin is a member of the M16 family of the clan ME zinc metalloproteases. This family of metalloproteases is characterized by an inverted active site motif of HXXEH. The two histidine residues and glutamate residues C-terminal to this motif are involved in coordinating a catalytic zinc ion (37, 38). Falcilysin is unable to cleave native hemoglobin or denatured globin, instead preferring to cleave small globin peptides up to 20 amino acids in length (39). It appears that falcilysin acts as a complement to the plasmepsins and falcipains, acting downstream, and cleaving

preferentially at polar residues, while plasmepsins and falcipains cleave at hydrophobic residues (*40*). The cleavage of globin peptides by facilysin is essential for production of peptides small enough to be transported to the cytosol of the parasite for further cleavage to amino acids, signifying the end of hemoglobin degradation in the digestive food vacuole.

During this process of hemoglobin degradation, large quantities of free heme are released and can reach concentrations of 400 mM if heme detoxification is prevented (40). The presence of free heme within the digestive food vacuole has several undesirable consequences. Heme concentrations as low as 10-20 µM have been shown to inhibit several proteases present within the digestive food vacuole including the plasmepsins and falcipains (40). In addition to inhibiting enzymatic activity, the presence of free heme is detrimental to the stability and deformability of the parasite vacuolar membrane (15). The resulting hemolysis is likely caused by perturbations to the membrane structure from the insertion of lipophilic heme into the phospholipid bilayer. A further consequence of free heme accumulation is the increase in oxidative stress on the parasite (41). Since the malaria parasite does not have HO like vertebrates, the parasite detoxifies free heme by converting soluble, toxic free heme into an insoluble, nontoxic crystal called hemozoin. This process is essential to parasite survival, as inhibition of hemozoin formation results in parasite death (42). Indeed, the most successful antimalarial ever developed, chloroquine, has been shown to inhibit this detoxification pathway supposedly by binding free heme and preventing its insertion into the growing hemozoin crystal. Unfortunately, due to resistance mechanisms

developed by the parasite, chloroquine no longer has clinical efficacy. However,

hemozoin remains a valid drug target as resistance is a result of efflux, and resistant

strains of the parasite still produce hemozoin normally. Therefore, it is essential that

the formation of this biocrystal is better understood in order to promote the discovery

of new antimalarials that target hemozoin formation.

The Structure of Hemozoin

Lancisi reported the discovery of hemozoin, the dark brown-black malarial

pigment, in 1717 (43). As these deposits are quite pronounced in the brains, spleens and

livers of malaria victims, the discovery of hemozoin actually precedes the discovery of

the malaria parasite itself by over 150 years. For many years, it was hotly contested as

to whether or not pigment was the actual cause of malaria, but in 1890, Golgi presented

a photograph of a pigmented parasite in the blood of a malaria patient, forging the

connection between hemozoin and malaria (15, 44). The composition and structure of

hemozoin remained a subject of intense debate until 2000 when X-ray powder

diffraction methods were used to identify the structure of β-hematin, the synthetic

equivalent of hemozoin (45). Once thought to consist of polymeric strands of O-Fe(III)

linked heme units, XRD revealed a centrosymmetric triclinic unit cell comprised of

reciprocal head-to-tail dimeric units of heme bound through propionate O-Fe(III) with a

bond distance of 1.866(2) Å (Figure 3). The propionic acid groups of the heme dimer

then hydrogen bond with other dimers to form the extended crystal. Morphologically,

β-hematin and hemozoin crystals are needle-like and exhibit dominant, slow growing

{100} and {010} side faces with minor, less pronounced fast growing {011} and (46) end

faces (Figure 4). This morphology is conserved among various species of *Plasmodium*

(Figure 5).
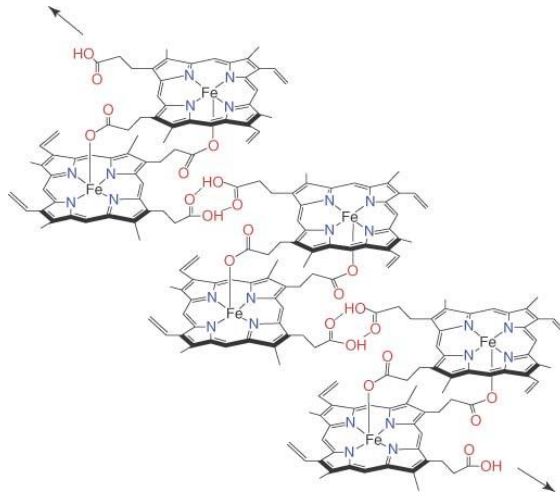
Figure 3. Structure of Hemozoin
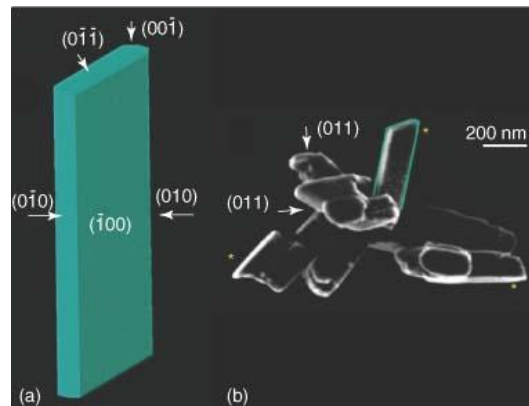
Figure 4. Crystal morphology of hemozoin showing slow-growing {100} and {010} side faces, and fast-growing {011} and {46} faces.
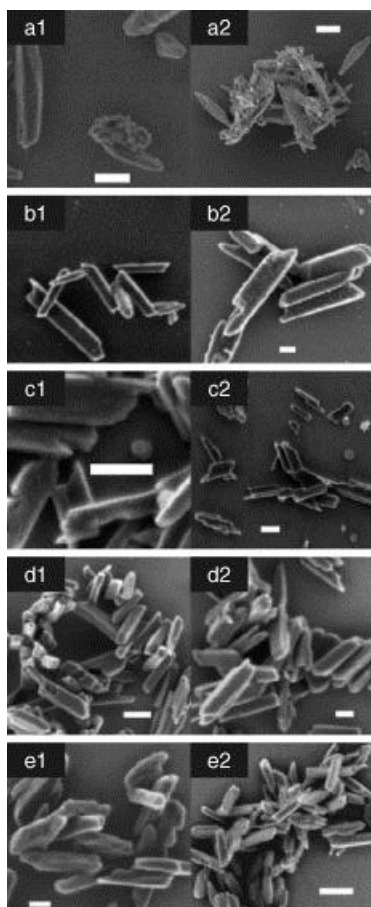
Figure 5. Electron micrographs show the heterogeneity of shape and size for B-hematin and hemozoin. Images of B-hematin (a) compared to that of hemozoin from *P. falciparum* clones Dd2 (b1) and 3B-D5 (b2), and hemozoin from *P. Vivax* (c), *P. ovale* (d), and *P. malariae* (e). The size bar is 200 nm (50).

Hemozoin and β-hematin are equivalent

Understanding the mechanism by which the parasite converts soluble, toxic free heme into an insoluble and non-toxic crystal is valuable for antimalarial drug-discovery, as perturbations to this crystallization process can result in parasite death. However,

studying the formation of hemozoin *in vivo* has proven challenging to researchers. β-hematin (BH), the abiological version, has been utilized as a tool to study hemozoin formation *in vitro*. For such comparisons to be meaningful, it had to be unequivocally established that these entities are isostructural. Chemical, spectroscopic, and crystallographic evidence have been used to conclude the similarity of these two materials.

Chemically, both hemozoin and BH are composed of insoluble, head-to-tail dimers of Fe(III)PPIX (47). Spectroscopically, the similarity of hemozoin and BH dimeric units can be confirmed from the infrared spectrum, that exhibits fingerprint vibrations around 1664 and 1211 cm^{-1} corresponding to the C=O and C-O stretching from coordination of the propionate O atom to the Fe(III) metal center of the neighboring heme molecule (48). Furthermore, the Fe(III) spin state of each species is identical, confirmed by variable temperature EPR that has shown that both BH and hemozoin exist in the high spin S=5/2 state, a paramagnetic complex. This observation is in agreement with Mössbauer data where the isomer shift and quadrupolar splitting values suggest that the Fe(III) exists in a high-spin state (47, 49). Morphologically, SEM images reveal that both BH and hemozoin are composed of needle-like crystals with tapered habits (Figure 5A and 5B). The crystal structure of each species is nearly identical. Synchrotron x-ray powder diffraction patterns have demonstrated that the crystal structure of hemozoin is identical to its synthetic counterpart (50). However, a more recent study suggests hemozoin may contain slightly more disorder in the Fe-O bonds than BH formed under nonaqueous equilibrium conditions (51).

Mechanism of Hemozoin Formation

The conversion of free heme to BH does not occur at a physiologically relevant rate in aqueous solution, suggesting that the *in vivo* formation of hemozoin within the digestive food vacuole of the parasite requires the presence of a biological mediator. While the precise mechanism by which hemozoin formation occurs *in vivo* is not fully elucidated, recent studies strongly support the hypothesis that neutral lipid bodies are the biological template for hemozoin crystallization. In support of this hypothesis, several synthetic routes for BH formation have been described demonstrating that neutral lipid bodies serve as both a protective reservoir for free heme and a kinetically competent site for crystallization.

Biological formation of Hemozoin

Until recently, identification of the biological mediator responsible for hemozoin formation was a controversial topic, as proteins, membrane lipids and neutral lipids extracted from the *Plasmodium* parasite were each shown to mediate BH formation *in vitro*. Indeed, many biological components within parasite lysates are quite capable of promoting the formation of BH *in vitro*. One of the earliest studies of these lysates was conducted by Slater and Cerami who examined trophozoite extracts (52). The formation of BH in the presence of these extracts was dependent on pH, time and concentration. Furthermore, several quinoline-antimalarials (known to inhibit the formation of hemozoin *in vivo*) were found to inhibit the process of BH formation in the presence of these lysates. The authors concluded that the presence of an enzyme, a heme

polymerase, was responsible for mediating the formation of BH, as activity of these

lysates was sensitive to both heat and treatment with 1% SDS. However, subsequent

work contradicted this hypothesis, demonstrating that heat treated parasite lysates

retained activity and therefore are not dependent on the presence of an enzyme (49). It

was suggested that BH formation in these experiments was actually due to the presence

of hemozoin crystals within the lysates. In fact, the authors showed that preformed BH

crystals were sufficient to seed the process of crystallization *in vitro*. While these

studies demonstrated that an enzyme is not necessary for hemozoin formation, the

mechanism of hemozoin crystallization remained unanswered.

Polar membrane lipids were also implicated as a possible mediator of hemozoin

formation. Bendrat *et al*. first implicated these polar lipids when acetonitrile extracts of

authentic hemozoin were found to promote the formation of BH (53). MS analysis of

these extracts identified the presence of the methyl esters of oleic, palmitic and stearic

acids and low yields of phospholipids within the active fractions. Further, it seemed that

these studies were in agreement with a previously published TEM image of an intact

parasite showing aligned parallelepiped crystals of hemozoin present within the DV of

the parasite (54). These observations supported the hypothesis that crystallization

occurs via epitaxial nucleation of hemozoin at the lipid layer of the vacuolar membrane

(55). Despite the strength of this argument, it was later revealed that axenic parasite

cultures lacking a parasitophorus vacuolar membrane still produce hemozoin, ruling out

any role for these membrane lipids in the parasite's mechanism of heme detoxification

(56). While these polar membrane lipids are capable of promoting BH formation *in vitro*, they are not responsible for the *in vivo* formation of hemozoin.

Though polar membrane lipids were ruled out as the mediator of hemozoin formation, additional studies by Dorn *et al*. showed that extracts from uninfected erythrocytes as well as several types of phospholipids are also capable of promoting the formation of BH (56, 57). These observations suggest that a hydrophobic environment is ideal for promoting formation of BH. Several *in vitro* studies substantiate this hypothesis by probing both the rate and activation barrier of BH formation in the presence of several types of solvents, alcohols and acids with varying degrees of hydrophobicity (58). Several acids, including benzoic and acetic acid have been shown to mediate BH formation (59). The ability of the acid to promote BH formation increases as a function of concentration. It has been suggested that this concentration dependence is due to an increase in heme solubility, the limiting step in BH formation. This observation would explain the abundance of active BH mediators obtained from lipophilic biological extracts. As heme itself is quite hydrophobic and insoluble in aqueous solution, it would be expected that heme solubility would increase of a function of increasing hydrophobicity of the surrounding environment.

Following this line of thinking, aromatic and aliphatic alcohol-water mixtures of varying hydrophobicity have been studied for their ability to promote BH crystallization (60-62). In one such study, the ability of several small normal and structurally similar alcohols with varying degrees of hydrophobicity were investigated (61). The results indicate that activity follows the trend of butanol > propanol > ethanol > methanol.

These data suggest that the hydrophobicity of the alcohol is directly related to its potency as a mediator of BH formation. The authors further investigated the solubilization of heme in the presence of the alcohols and found an exponential increase of heme solubility is observed as a function of increasing alcohol concentration. Further, the ability of an alcohol to solubilize free heme followed the trend of proponal > ethanol > methanol indicating that the hydrophobicity of the alcohol increases the solubility of heme. These data would support the concept of an *in vivo* mediator of hemozoin formation that is hydrophobic in nature and acts to solubilize free heme.

In vitro experiments have shown that BH formation occurs efficiently at the surface of a hydrophilic/hydrophobic interfacial region. These observations were made using aqueous/alcohol mixtures in the presence or absence of an interfacial region (63, 64). To study the effects of this interfacial region, a cosolvent system was implemented where a 9:1 solution of methanol:alcohol was used. In the case of 1-octanol, 1-hexanol and 1-pentanol, the first two solvents are biphasic in aqueous medium, while the latter exhibits a single phase in aqueous solution. The rates of formation of BH at physiological temperature and digestive food vacuole pH for the solvent systems are 7-9 minutes for the biphasic solutions, but 110 minutes for the 1-pentanol solution, which could suggest that the presence of an interfacial region is important. To confirm the importance of this lipophilic interface, a solution of 6:4 methanol:pentanol or octanol was used, so as to induce an interfacial region in the pentanol solution. The results show that the 1-octanol solution has a similar half-life (12 min) as observed in the 9:1 solution (7.1 min). However, the 1-pentanol solution with an interfacial region shows a

half-life of 10 min, as compared to the kinetics in the absence of an interface where the half-life is 110 min. Another study with resonance raman spectroscopy using an immersion probe confirmed that the formation of BH occurs within 1 μm of a pentanol/water interface. Due to the dependence of BH formation on the presence of an interfacial region, perhaps formation of hemozoin at a lipid/aqueous interface explains the alignment of crystals on neutral lipid bodies observed in TEM images.

These *in vitro* experiments demonstrate that hydrophobic interactions are important in free heme detoxification, suggesting that a lipophilic source present within the digestive food vacuole is responsible for mediating hemozoin formation. Since polar membrane lipids have been previously ruled out, is there another possible lipophilic source present at the site of hemozoin formation? With the identification of neutral lipids bodies present within the digestive food vacuole, the focus shifted to these neutral lipids as the possible site of hemozoin formation.

Implication of Neutral Lipids in Hemozoin Formation

During infection with *P. falciparum*, there is a six-fold increase of lipid content within the erythrocyte for the support of growth and differentiation of the parasite. While the parasite does support limited synthesis of short chain fatty acids, the lipid content of the growing parasite is mostly scavenged from the host. During this process, there is a significant increase in triacylglycerol content, a neutral lipid that is only detected in small amounts within an uninfected erythrocyte. Within the digestive food vacuole of the parasite, aggregates of these neutral lipids are observed. Confocal

images reveal these lipid bodies are a few hundred nm in diameter and determined to consist of a mixture of di- and triacylglycerols (neutral lipids) (64). Based on previous knowledge that mono- di- and triacylglycerols are capable of promoting BH formation, it was proposed that the neutral lipid bodies serve as a mediating template for the formation of hemozoin (48). Later, Sullivan and coworkers revealed a TEM image clearly showing crystals of hemozoin aligned along the surface of these lipid bodies, thereby strengthening the role of these hydrophobic bodies in hemozoin formation (Figure 6) (65).
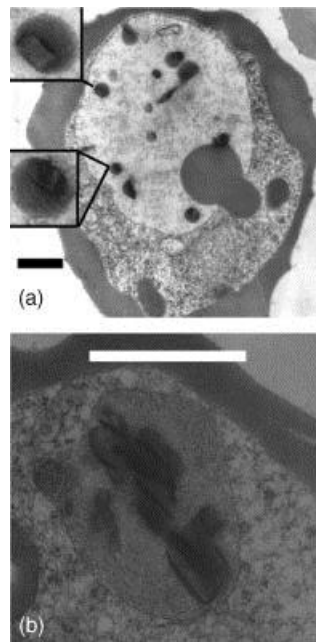

Figure 6. (a) hemozoin formation within lipid droplets is observed with malachite green fixation. (b) Formation of hemozoin crystals within a lipid droplet. Seen with malachite green fixation (65).

In an attempt to identify the specific composition of these neutral lipid bodies, the authors extracted the digestive food vacuole of the parasite and performed lipid analysis using ESI-MS/MS (electrospray ionization tandem MS) on the hemozoin extracts. The results showed that the lipid composition surrounding the hemozoin crystals are composed of a specific ratio of neutral lipids in an approximate ratio of 4:2:1:1:1 of MSG (monostearic glycerol), MPG (monopalmitic glycerol), DPG (dipalmitic glycerol), DOG (dioleic glycerol) and DLG (dilinoleic glycerol). The authors investigated the kinetic formation of BH in the presence of this blend of neutral lipids and revealed that BH crystallization occurred within ten minutes of incubation with linear growth for 2 h before reaching 80% product conversion. The authors also provided evidence that the neutral lipid bodies help protect heme from peroxide degradation, which would lead to parasite toxicity. In the absence of these lipids, a 50 mM H_2O_2 solution degraded 50% of dilipidated hemozoin, while a 90 mM concentration of peroxide was necessary to reduce encapsulated hemozoin by 50%, suggesting that the lipids may also serve as a protective reservoir for free heme preceding its incorporation into the nontoxic hemozoin crystal.

Localization of free heme in the neutral lipid body

This interpretation of the lipid body serving as a reservoir for free heme is supported by *in vitro* confocal evidence (66). Fluorescently labeled synthetic neutral lipid bodies (SNLDs) were generated by dissolving the biological blend of neutral lipids in 1:9 acetone:methanol in the presence of Nile Red. When added to a pH 4.8 citric buffer,

the hydrophobic lipids minimize interactions with water by forming spherical, continuous hydrophobic bodies, very similar to those observed within the native environment of the parasitic digestive food vacuole. As these SNLDs are formed, Nile Red becomes trapped within the hydrophobic environment, and any Nile Red not enveloped within the SNLDs will be quenched by water. The resultant fluorescent SNLDs can be visualized using confocal microscopy (Figure 7). This system was then titrated with heme, which quenches Nile Red in a concentration dependent manner. At pH 4.8, it is observed that free heme rapidly partitions throughout the lipid body from the outside-in. Complete quenching is observed in 200 seconds. However, at pH 1.3 and 7.3, quenching is much slower and appears to associate with the near surface layer of lipids (Figure 8a). The partitioning of free heme as a function of pH follows a bell-shaped curve, with maximal heme partitioning observed at digestive food vacuole pH 4.8. Importantly, the pH dependence of the yield of BH formation follows the same trend, indicating that BH formation occurs as a function of heme partitioning into the SNLDs (Figure 8b).
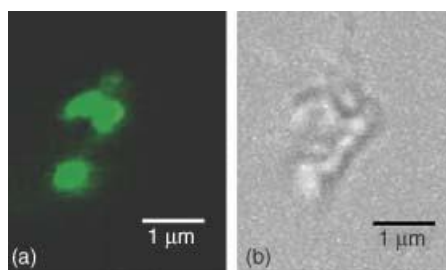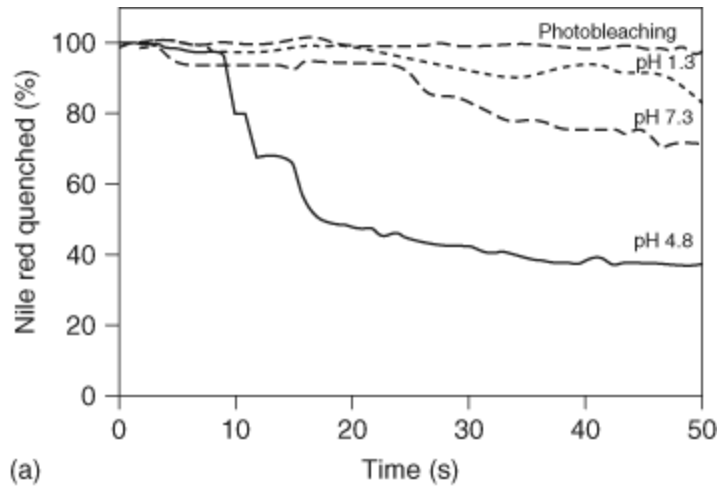

Figure 7. (a) Confocal microscopy images showing neutral lipid droplets containing Nile Red. (b) As the droplets were titrated with heme, the Nile Red fluorescence was quenched, indicating that free heme partitions into neutral lipid bodies.
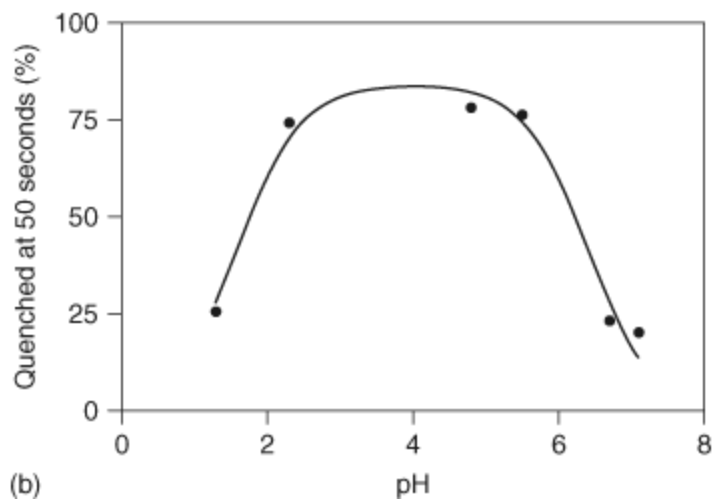
Figure 8. (a) Comparison of Nile Red quenching as a function of time at different pH. (b) Partitioning of free heme as a function of pH follows a bell-shaped curve, with maximum partitioning occurring at 4.8.

Kinetically competent site for BH formation

It has been estimated that the maximum half-life required for hemozoin conversion must be no more than 40 minutes in order for the parasite to escape free heme toxicity (67). If the neutral lipid body is imagined to be a reservoir for toxic heme, then it must be capable of promoting the formation of hemozoin at a kinetically

competent rate. Recently, an *in vitro* study that mimics digestive food vacuole conditions has established the ability of these SNLDs to mediate the formation of BH (68, 69). SNLDs were created in a pH 4.8 citric acid buffer at 37°C. An aliquot of Fe(III)PPIX was then added to the SNLDs in order to determine the half-life of BH formation. The product obtained was then crystallographically verified to be equivalent to hemozoin. In the biologically relevant 4:2:1:1:1 ratio SNLDs, the half-life of BH formation was 1.9 ± 0.01 min, demonstrating that the neutral lipid blend is capable of successfully detoxifying free heme at a physiologically realistic rate that would protect the parasite from toxicity.

Significance of the blend of neutral lipids

Based on the wealth of data that supports BH formation in a lipophilic environment, it is not surprising that these neutral lipid bodies would be the *in vivo* location of hemozoin formation. It is interesting, however, that the parasite uses the specific blend of mono- and di-acylglycerols in the 4:2:1:1:1 ratio. Does this unique blend of neutral lipids offer an advantage over utilizing individual lipid components? To probe this question, temperature dependent kinetic measurements have been undertaken to determine whether the neutral lipid blend offers a lower activation barrier for BH formation over the individual lipid components (70, 71). For these experiments, SNLDs of each individual lipid component and the biological mixture (100 μM) were synthesized followed by the addition of Fe(III)PPIX. Kinetic observations were made to determine the half-life of BH formation as a function of time (Figure 9b). The

resulting data was fit to the Arrhenius equation and the activation energy was

determined (Figure 9c). The activation barriers for MSG, MPG, DOG, DLG, and DPG were

74.8 ± 5.3, 60.4 ± 7.1, 37.7 ± 3.3, 44.5 ± 15.4 and 35.2 ± 9.4 kJ/mol, respectively. These

results show that the monoglycerides exhibit an energy barrier that is higher than

observed for the diglycerides. However, in the neutral lipid blend (final concentration

100 µM) the activation barrier is 27.8 ± 3.4 kJ/mol (Figure 9a), lower than that of any of

the individual lipid components.
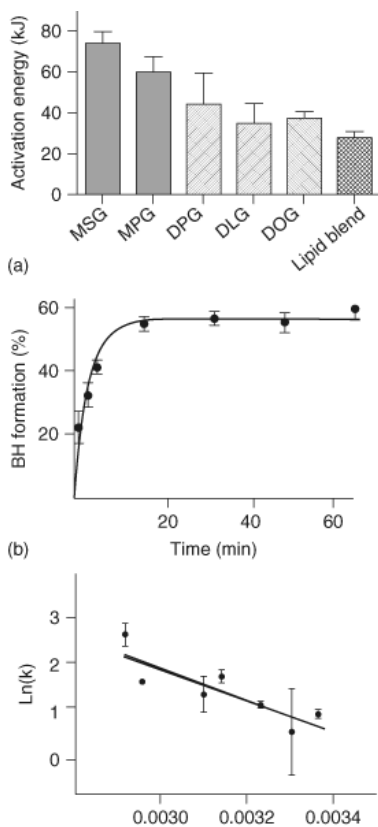
Figure 9. (a) Activation energy of neutral lipid blend, and separate mono-, di-glycerides. (b) half-life of BH formation as a function of time. (c) Activation energy was determined by the Arrhenius Equation.

This lower activation barrier suggests that the lipid blend offers an advantage compared to using an individual lipid component. Recognizing this difference, Hoang *et al.* further examined these lipids to identify whether or not the lipid blend exhibited properties that are unique from the individual lipid components. Using differential scanning calorimetry (DSC), a thermoanalytical technique that detects phase transitions by measuring the heat flux of a sample, it was discovered that new intermolecular interactions are observed in the lipid blend that are not present within the individual components, demonstrating that the blend has a different molecular organization than the individual components.

Molecular Dynamics Simulations

In addition to experimental data that suggests hemozoin formation occurs in the presence of neutral lipid bodies, molecular dynamics (MD) simulations have further shown that crystallization would be supported in this lipophilic environment (67-69). In MD in vacuum, the interaction of two H_2O-Fe(III)PPIX molecules form a precursor to the head to tail dimer (Figure 10) in which the propionate groups interact with the corresponding Fe(III) center. A ligand exchange then occurs with the displacement of the water ligand from the axial position of Fe(III) and formation of the Fe-O bond. Rapid hydrogen bonding between the propionic groups of dimers then occur. In these simulations, if water molecules are present with the precursor dimer, the propionate groups move away from the Fe(III) center to interact with the water molecules. These simulations would suggest that the neutral lipid body serves as a hydrophobic

environment that minimizes the interactions with water molecules and drives formation of the hemozoin crystal.
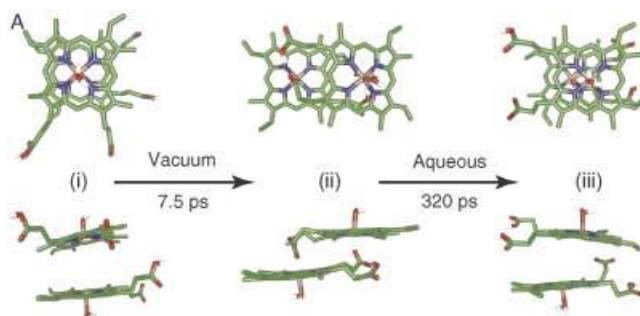

Figure 10. Molecular Dynamics (MD) simulation of hemozoin formation

No single piece of evidence presented here alone could unequivocally implicate neutral lipids in heme detoxification *in vivo*. However, collectively, a role for neutral lipid bodies in hemozoin formation is undeniable. Not only has confocal evidence shown that heme spontaneously localizes within these neutral lipid bodies, but they also serve as a kinetically competent site for hemozoin formation. Previous evidence showing hemozoin encapsulated within these neutral lipid bodies provides convincing evidence that this is indeed the site for hemozoin formation within the digestive food vacuole. MD studies further substantiate the likelihood that hemozoin formation occurs at this site. It is clear that free heme accumulates within the neutral lipid body, and that the lipid bodies are sufficient to quickly detoxify free heme on a physiologically relevant time scale. The rapid formation of the head-to-tail dimer is favored in the lipophilic

environment and would not be expected to occur rapidly in aqueous solution due to competitive hydrogen bonding.

Antimalarials

The malaria parasite contains several unique metabolic pathways which may be exploited for the discovery of new antimalarials. These include targeting the synthesis of DNA precursors (69), fatty acid synthesis (71), glycolysis (72) , and de novo heme biosynthesis (73), among others. Of relevance here, however, is inhibition of the formation of hemozoin. One of the earliest effective treatments for malaria dating from the 17th century (74) was prepared from bark of *Cinchona* spp., The most active component of "Jesuit's bark" was later identified as quinine, a potent inhibitor of BH formation (75). Chloroquine, arguably the most successful antimalarial developed to this day, is an analogue of quinine and is thought to share a similar mechanism of action: inhibition of hemozoin formation. Unfortunately, the efficacy of chloroquine has widely diminished in endemic areas due to rampant drug resistance. These resistant strains of *P. falciparum* exhibit several mutations in the *Plasmodium falciparum* chloroquine resistance transporter (PfCRT), a transmembrane vacuolar protein. In resistant strains the accumulation of CQ within the digestive food vacuole is significantly less than in wild-type strains, as it is actively transported out of the DV (76). Nevertheless, hemozoin formation remains a valid drug target, as resistance is the result of diminished vacuolar accumulation of CQ, rather than changes to the hemozoin formation pathway itself. Importantly, the interactions of hemozoin and antimalarial

inhibitors of this pathway have been studied in great detail, lending a wealth of

information that can facilitate the drug discovery process.

Evaluating Small Molecule Interactions with Heme

In order to understand the mode of action of hemozoin inhibitors, it is critical to

understand possible interactions between these drugs and heme and or hemozoin.

These efforts have been hampered by the insoluble nature of heme in a physiologically

relevant environment. *In vivo*, the speciation of free heme preceding the formation of

hemozoin is not fully understood, however, *in vitro* experiments reveal that free heme

can exist as a monomer, or several different dimeric species depending on

environmental factors (Figure 11) (77). When investigating the interactions of heme

with BH inhibitors, it is essential to identify the dominate species of heme present in

solution as to facilitate a meaningful interpretation of the results. The primary dimeric

forms of heme that are observed in solution are the π-π backbonding dimer (likely the

most important species in hemozoin formation) (**I**), the μ-oxo dimer (**II**), and larger π

bonding aggregates of μ-oxo dimers (**III**). The distribution of these heme species *in vitro*

are reversible and can be regulated by careful control of the heme concentration, pH,

salt content and solvent system in solution (78). At very low concentrations of heme in

aqueous solutions or in the presence of a high percentage of organic solvent, heme can

be solubilized and will exist mostly in the monomeric form (**I**) (79). This species of heme

is important since monomeric heme would be the species of heme released during

hemoglobin degradation. At higher concentrations of heme in aqueous solution, the π-π

dimer (**II**) will dominate (*79*). This is also true for protic solvent mixtures, since the

conversion between μ-oxo dimer and the π-π dimer depend on the protonation of the

oxygen bridging atom. This π-π species is likely the dominant form of heme present in

the digestive food vacuole, so is perhaps the most important species of heme that

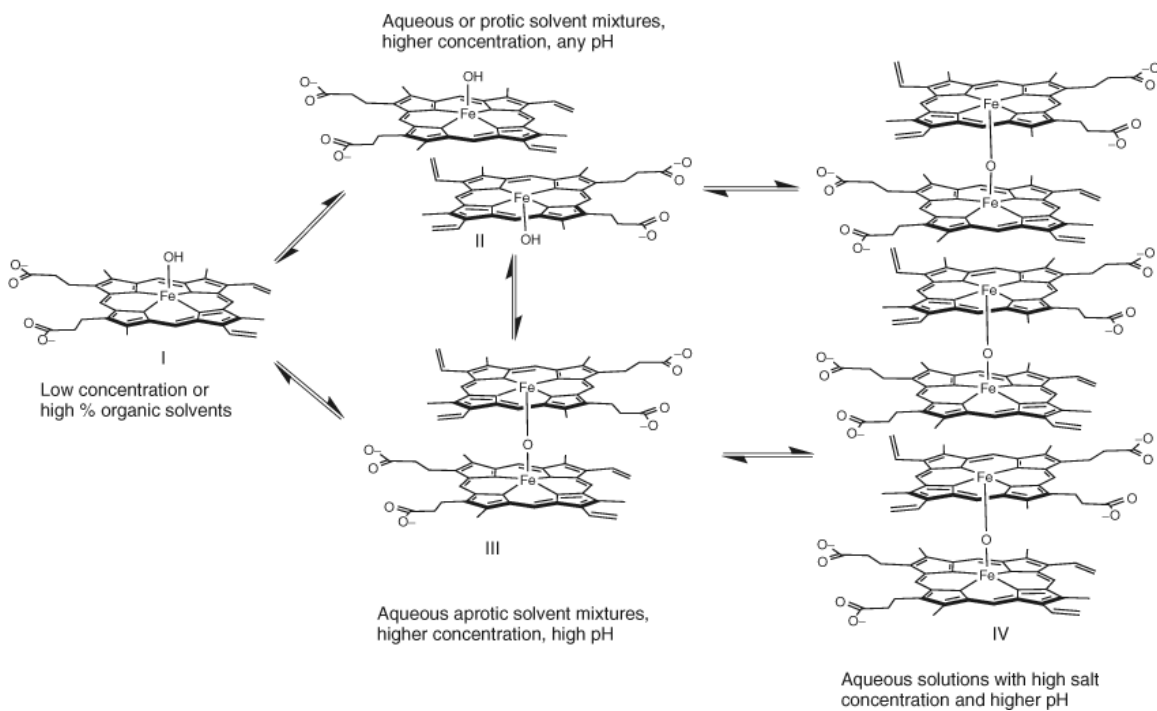should be studied in drug interactions.

Figure 11.Speciation of heme in different environments. Heme can exist as a monomer (I), a π-π dimer (II), a μ-oxo dimer (III), or as π bonding aggregates of the μ-oxo dimer (IV).

Vacuolar Accumeation

One of the confounding aspects of hemozoin inhibitors is that a compound's ability to inhibit the formation of β-hematin *in vitro* will not necessarily have a direct correlation to the *in vivo* inhibition of hemozoin unless the drug can successfully accumulate within the digestive food vacuole (DV) of the parasite at the sight of nucleation and crystallization. Consequently, targeting vacuolar accumulation is an important aspect of hemozoin inhibitor design. The primary mode that results in the accumulation of a drug within the DV is by 'pH trapping' as is observed in the mechanism of action of CQ, amodiaquine and mefloquine, among others. Here, lipophlic species that are neutral at physiological pH are capable of permeating cell membranes to gain entry into the malaria parasite. Upon entry into the digestive food vacuole, however, the species has entered an acidic compartment (pH 4.8). If protonatable functional groups are present (such as weakly basic functional groups), the species will become protonated and will no longer freely permeate the cell membrane, becoming trapped. This pH trapping drives the accumulation of antimalarials within the digestive food vacuole. In fact, using the known or calculated pK_a values for BH inhibitors, the vacuolar accumulation ratio (VAR) can be easily determined using a modified Henderson-Hasselbach equation (Equation 1) (79, 80).

Equation 1.

$$\frac{[Drug v]}{[Drug c]} = \frac{1 + 10^{(pka1 - pHv)} + 10^{(pka1 + pka2 - 2pHv)}}{1 + 10^{(pka1 - pHc)} + 10^{(pka1 + pka2 - 2pHc)}}$$

Using this idea of pH trapping, optimization of BH inhibitors using weakly basic functional groups could result in the accumulation of drug at the sight of action, which should reduce the IC$_{50}$ of the drug. This has been shown in the case of quinoline derivatives, where potency of the hemozoin inhibitor is increased as a function of increasing VAR. Therefore, compounds which are good inhibitors of BH formation but ineffective against *P. falciparum* could be potentially improved by the addition of weakly basic amine groups to improve vacuolar accumulation.

Antimalarials and Small Molecule Inhibitors of BH formation

Several antimalarial quinoline derivatives have been approved for human use including chloroquine, amodiaquine, mefloquine, primaquine and quinine (Figure 12), each of which is thought to act by inhibiting the formation of hemozoin. The arylmethanol class of compounds includes halofantrine and lumefantrine and has also been used for the treatment of malaria (Figure 12). Currently, none of these drugs are sufficient to combat the recurrence of malaria due to resistance, cost or adverse side-effects, resulting in a need for the discovery of new antimalarial drugs.

Aside from the potent quinoline derivatives, many other small molecules are known to inhibit the formation of BH, including derivatives of benzimidazoles, xanthones, quinazolines, phenanthrenes, methylene blue and benzofurans, to name a few (Figure 13). The reason for the potency of these chemical scaffolds varies, but generally occurs via π-π interactions of the compound with the aromatic porphyrin ring and/or direct coordination to the Fe(III) center of heme. Small molecule inhibitors of BH formation can interact not only with free heme, but also with the hemozoin crystal, or both, to inhibit formation of product. It is important to understand the interactions of an active compound with heme to facilitate the design and optimization of new antimalarials targeting the hemozoin formation pathway.
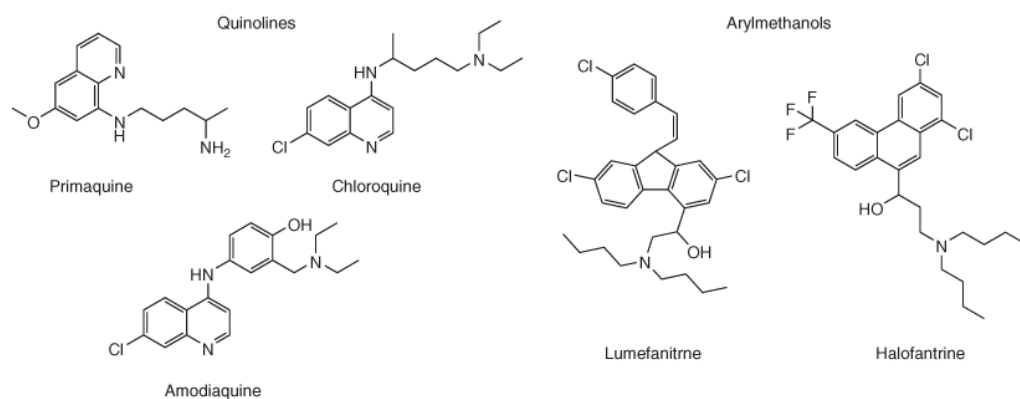

Figure 12. Structures of anti-malarial compounds of the quinoline and arylmethanol classes.
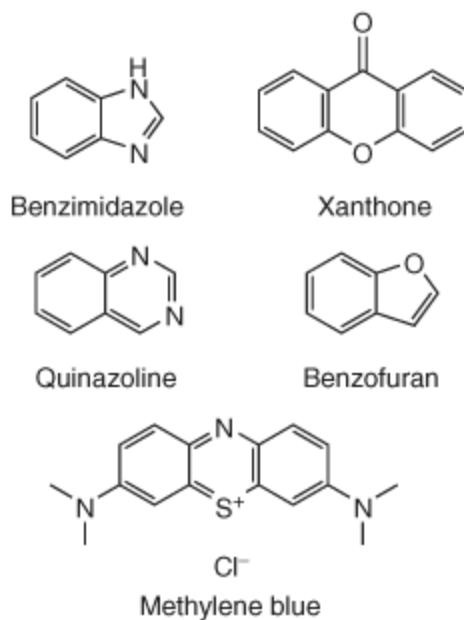
Figure 13. Structures of small molecule antimalarials.

Quinoline Derivatives

The interactions of many quinolines with heme have been documented. In the case of free heme, spectroscopic evidence supports that CQ, AQ and mefloquine (among others) interact with the porphyrin ring via π-π stacking with the quinloline ring (79). In the 1960's, it was first reported that CQ forms a complex with Fe(III)PPIX (81). Subsequent work in 1980 suggested that the targeting of heme by CQ may be the mechanism of action of the drug (82, 83). Spectroscopically, the interactions of free heme with CQ are well described (84). Upon titration of heme with CQ, there is a hypochromic shift in the soret band at 400 nm and a hyperchromic shift in the CT (charge-transfer) bands around 600 nm corresponding to the π-π interactions of CQ

with heme (85). Further support for the formation of a π-π complex is shown in the NMR spectrum of CQ following the addition of Fe(III)PPIX. The paramagnetic Fe(III) has a strong effect on the spectrum of CQ, where paramagnetic shifts are observed for both ^{1}H and ^{13}C (86, 87). Paramagnetic shifts and relaxation data indicate the presence of a π-π complex rather than a coordination complex.

It has also been proposed that some antimalarials such as the quinolines can absorb onto the surface of the hemozoin crystal itself, resulting in growth inhibition (88). When subinhibitory concentrations of {^{3}H}CQ were incubated with parasite cultures, electron autoradiographs of infected red blood cells revealed that the majority of the {^{3}H}CQ was colocalized with the hemozoin crystal (88). Later, a model of quinoline binding was proposed that suggested incorporation of CQ into the fast growing (89) corrugated faces of the crystal where grooves expose propionic acid groups, vinyl and methyl groups (90). CQ can intercalate the aromatic groups of the BH crystal and cap the (*48*) surface by forming a salt bridge between the quinoline amine and the propionic acid of the porphyrin, thereby inhibiting further growth of the crystal along this face. The CQ molecule would be further stabilized by interactions with the surrounding methyl and vinyl functional groups.

The ability of many of these quinoline derivatives to accumulate within the digestive food vacuole explains the potency of these drugs against wild-type strains of *P. falciparum*. For CQ, a percentage of this weakly basic, lipophilic quinoline derivative is neutral at physiological pH. The protonatable tertiary amine and quinoline nitrogen atoms of CQ have respective pK$_a$'s of 10.2 and 8.4. Consequently, as CQ passes into the

acidic (pH 4.8) DV, a portion of the drug becomes doubly protonated. The pH trapping

effect can be quite large. In CQ treatment, nanomolar concentrations of the drug in

plasma results in millimolar concentrations within the DV (89). This pH trapping effect

can be observed for other quinoline antimalarials including mefloquine and

amodiaquine.

Arylmethanol Derivatives

The arylmethanol family of compounds is another important class of quinoline

derived antimalarials that have been shown to interact with Fe(III)PPIX (48). This class

of compounds includes quinine, mefloquine, lumefantrine and halofantrine, among

others (Figure 13). Recently, the halofantrine-Fe(III)PPIX crystal structure was solved,

revealing that interactions occur with monomeric heme, but not dimeric heme (90).

The hydroxyl group of halofantrine coordinates directly to the Fe(III) center of heme

resulting in a five coordinate porphyrin complex. The hydroxide functionality of

halofantrine has a pKa of ~14 and would be expected to exist exclusively in the

protonated state in the acidic DV. However, the Fe(III)-O bond length (1.840(4) Å)

suggests the formation of an alkoxide bond (1.816 – 1.851 Å) and not an Fe(III)-alcohol

bond (2.113 – 2.160 Å). The depression of the hydroxyl pK_a may be due to the strong

coordination to the Fe(III) atom which induces a pK_a shift. Additionally, π-stacking of the

phenanthrene and porphyrin was confirmed. The unprotonated propionate of

Fe(III)PPIX interacts with both the protonated N atom of halofantrine and the propionic
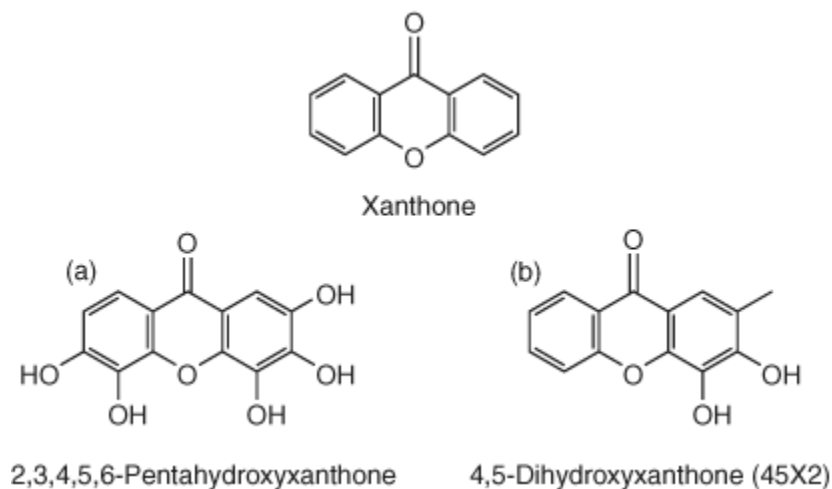
acid group of a neighboring heme.

Xanthones

Several other classes of BH inhibitors have been identified for potential use as

antimalarial drugs including the xanthones. Xanthones are known to exist naturally as

secondary metabolites primarily of the *Guttiferae* and *Gentianaceae* family of plants,

and were first identified for antimalarial activity by Riscoe and Winter (85, 91). Soon

after the discovery of the antiplasmodial activity of the xanthones, Ignatushchenko *et al.*

observed that these compounds exhibited stage specifity, noting that trophozoites were

more sensitive than were ring-stage parasites (92). This observation followed studies

that hypothesized heme as the potential drug target of these compounds (93, 94). It was

also shown that the xanthone derivative 2,3,4,5,6-pentahydroxyxanthone (Figure 14a)

formed a soluble complex with free heme. Later, the interactions between 45X2 (Figure

14b) and heme were examined in detail using NMR spectroscopy (93). These studies

demonstrated that the xanthone carbonyl moiety coordinates to the Fe(III) center of

heme. Further, hydrogen bonding between the hydroxyl groups of 45X2 and the

propionate side chains of heme were observed in addition to π-π stacking of the

aromatic regions of both species. The ratio of xanthone:heme was found to be 1:2 for

45X2. Since the discovery of xanthone activity against the parasite, studies have sought

to increase the potency of these compounds. The 3,6-bis-ω-

diethylaminoalkoxyxanthone class of xanthone derivatives developed by Kelly *et al.*

boasted an increased affinity for heme binding that resulted in an increased potency

against the parasite (95).

Figure 14. Structures of Xanthone and antimalarial xanthone derivatives

Artemisinin

This sespuiterpene trioxane lactone contains a peroxide bridge, which is crucial

to its activity (96). In the presence of this drug, heme acts both as an activator and a

target of artemisinin free radicals. As an activator, heme catalyzes the opening of the

peroxide bridge of artemisinin, thereby promoting the formation of carbon-centered

free radicals (97). The resultant radicals cannot be cyclically oxidized and reduced (98),

therefore only one free radical can result from a single drug molecule. Instead of being

cyclically regenerated, the radicals form covalent bonds with targets. Heme is also an

important target of alkylation by artemisinin free radicals, where the free radicals have

been found to form covalent bonds with heme. Artemisinin free radicals also form

covalent adducts with certain parasite proteins including the heme-binding

37

translationally controlled tumor protein (TCTP), and in membrane containing structures including the plasma membrane, endoplasmic reticulum, nuclear envelope, digestive vacuole membrane, and mitochondria (99-102). Because artemisinin and its derivatives are activated by free heme, it represents a very parasite specific malaria treatment.

High-Throughput Screening and Drug Discovery

With parasite antimalarial resistance on the rise, there is a pressing need for the discovery of novel chemical scaffolds that are active against *Plasmodium* spp. One discovery technique is high-throughput screening (HTS), where thousands to millions of small molecules are rapidly tested for activity in assay. An HTS suitable assay is generally formatted for use in 384- or 1536-well microtiter plates in order to test a large quantity of compounds in a small amount of time. Furthermore, an HTS amenable assay must involve minimal processing steps, be highly robust and should be comprised of easily accessible reagents at a minimal cost. Assays can be either phenotypic or target-based in nature. In antimalarial HTS, phenotypic assays are those that seek to identify small molecules that are capable of killing the parasite itself in *P.falciparum* infected erythrocytes. The disadvantage to this approach is that the mechanism of action of inhibitors is unknown, and can be quite difficult to elucidate. In target-based assays, a specific cellular process, such as hemozoin formation, is used to identify potential antimalarials. Inhibitor/target interactions can be studied immediately after identifying hits, an advantage over phenotypic screening. An additional advantage is the option to

select pathways that are specific to the parasite. The disadvantage to target-based screening is that activity does not necessarily confer to the whole-cell assay.

The use of HTS in antimalarial drug discovery has been utilized in recent years for both target-based and phenotypic assays (103). Of the target based assays, several have been developed for the purpose of identifying inhibitors of BH formation (104-108). One of the first successful assays developed for use in HTS utilized radioactive ^{14}C-labeled hematin to quantitate BH formation using scintillation counting (109-114). Crystallization was mediated by the addition of lipid-rich extracts from parasite lysates. The semi-automated assay tested over 100,000 compounds in 96-well plates and identified 45 nonquinoline hits. Of these 45 compounds, the structural classes of compounds identified included triarylcarbinols, piperazines, benzophenones, imides, hydrazides, indoles and isoxazoles. The non-quinoline hits were then tested in a secondary whole-cell assay consisting of cultures of CQ-sensitive and CQ-resistant *P. falciparum.* Four compounds were identified to have activity in both strains at concentrations of <5 µM (the IC$_{50}$ of CQ in sensitive strains of *P. falciparum* is ~25 nM). Though few of the compounds identified in the BH inhibition screen were active against parasite cultures, the ability of HTS to identify novel pharmacophores supported the utility of this approach. However, this assay was not utilized to its full potential due to deficiencies in design. The semi-automated use of 96-well plates would be considered a medium-throughput method compared to the more often used 384- and 1536- well plates. Further, the need for trophozoite lysates and radioactive hematin limits the use of this assay to laboratories capable of maintaining parasite cultures and open to the

restrictions imposed by utilizing radioactive substrates. Fortunately, subsequent BH

formation assays have improved upon the original protocol by increasing the

throughput of compound screening, incorporating more readily available substrates,

and using improved methods of quantification that do not require the use of radio-

labeled heme.

In 2009, Clardy and coworkers developed a true HTS assay that utilizes acetate

buffer for the synthesis of BH in 384-well microtiter plates (113, 115, 116). In this assay,

a high concentration (9.7 M, pH 4.8) of sodium acetate buffer is utilized to mediate the

formation of BH by solubilizing Fe(III)PPIX, the rate limiting step in BH formation. The

assay is incubated at 60°C for 120 min, then analyzed using the pyridine ferrichrome

method of quantification developed by Egan and coworkers (114). Using this assay to

screen 16,000 compounds at a 220 µM concentration of test compound, 644 hits (3.96%

hit-rate) capable of inhibiting >50% BH formation were identified. Of these 644 hits, 17

were identified as active against *in vitro* cultures of *P. falciparum* (hits were identified as

having activity of >80% against the parasite). As a direct result of this screening effort,

the authors identified two novel classes of compounds that show activity in both the BH

formation assay, as well as the whole-cell parasite assay. Two classes of compounds,

the pyrimidine and 1,3-benzoxathiol-2-one compounds were identified in this screen.

While this assay was a major improvement upon previously published medium-

throughput assays, the conditions for BH formation were not physiologically relevant.

This is perhaps the reason that so few of the BH inhibitors show activity against cultures

of *P. falciparum*.

Improved understanding of the *in vivo* formation of hemozoin has facilitated

advances in HTS assay design for the discovery of novel BH inhibitors. Of vital

importance is the identification of neutral lipids as playing a role in hemozoin formation

(117). The composition of these lipids has been found to mediate the formation of BH

and is inhibited upon co-incubation with the quinoline antimalarials. Due to the

relatively high cost of these neutral lipids, they are not practical for use in HTS. An

alternative is the use of commercially available, low cost detergents, several of which

have been shown to mediate formation of BH in 96- and 384-well plate format in vitro

and in HTS formats (116) (65). The assay uses the lipophilic detergent, NP-40, to

mediate BH crystallization at a pH of 4.9 (116, 118). Further, when co-incubated with

CQ or AQ, NP-40 exhibits similar IC_{50}'s to those obtained when using the neutral lipid

blend. Using this assay, a pilot screen of over 38,000 compounds resulted in the

identification of 161 hits, a 0.42% hit-rate. IC_{50} values were obtained for each of these

hits and included the identification of 113 compounds with lower IC_{50} values than that

of AQ in this assay. These compounds were then tested for efficacy against *P.falciparum*

infected erythrocytes and 48 compounds were identified as capable of inhibiting >90%

of parasitemia, including the identification of eight compounds with activities at

nanomolar concentrations (Figure 15a). Four distinct chemical scaffolds were identified

(Figure 15b).

Structure	BH IC50 (μM)	MSF IC50 (nM)
	5.9	194
	14.3	348
	6.2	46
	12.9	38
	15.1	49
	12.1	65
	12.6	310
	29.1	590

(a)

(b)   I   II   III   IV

Figure 15. (a) Structures of antimalarial compounds found to be active in the malaria parasite, and (b) four distinct chemical scaffolds.

Conclusion

In order to survive, the malaria parasite relies on a unique detoxification pathway in which toxic free heme is converted to the nontoxic biomineral hemozoin. Disruption of this crystallization process results in parasite death, and therefore serves as an important strategy for drug design. Hemozoin formation does not occur

42

spontaneously at a physiologically relevant rate, and identification of the biological mediator of this crystal remained elusive for many years. Recently, neutral lipid bodies present within the digestive food vacuole of the parasite have been replicated *in vitro* (SNLDs). It has been found that Fe(III)PPIX rapidly accumulates within these SNLDs. Furthermore, the SNLDs have been shown to serve as a kinetically competent site for BH formation. These data demonstrate that the neutral lipid bodies are the biological mediator of hemozoin formation. Using this information, an assay that mimics the physiological environment in which hemozoin formation takes place has been developed and used in high-throughput screening to identify novel inhibitors of this target. Furthermore, the interactions of hemozoin inhibitors with free heme have been studied in detail. These studies have revealed that inhibitors can interact through π-π interactions and/or direct coordination to the Fe(III) center, inhibiting the incorporation of the heme into the growing hemozoin crystal. The information gained from these interactions can now be used to optimize compounds that inhibit BH formation. All of these advances have only been made possible by first understanding the formation of the biomineral, hemozoin.

Chapter II

Isolation of Anti-malarial Compounds from a Natural Product Library

<u>Introduction</u>

Natural products have long been the single most productive source of leads for

drug development (*119*). Between 1981 and 2002, 49% of all small-molecule New

Chemical Entities (NCEs) were natural products, natural product analogues, or natural

product derivatives (*120*). In fact, the anti-malarial drug chloroquine is derived from

quinine, a natural product found in the bark of the Cinchona tree (See figure 12).

Despite the success of natural products in the drug discovery field, the emphasis on

natural product drug discovery has waned in the past decade for several reasons.

First, the emergence of combinatorial libraries and their promise of many

potential biologically active compounds, short timelines, and high-throughput

capabilities took the focus away from the slow process of natural product purification,

screening, structure elucidation, and subsequent scale-up (*119*). Secondly, the increase

in molecular biology, genomics, and cellular biology techniques made the discovery of

new drug targets possible, increasing the demand for shorter drug discovery timelines.

Finally, the reduction of emphasis on infectious disease research - a typical strong point

of many biologically active natural products - encouraged scientists to move from

natural product screening to screening much larger, synthetic libraries (*120*).

Utilizing the new technologies born from the combinatorial chemistry drug discovery era, science is once again turning to natural product drug discovery to produce useful biologically active compounds. Many bioactive compounds discovered previously have come from a class of soil bacteria called actinomycetes. This class of bacteria has been the main producer of approved antibiotics and other biologically active metabolites to date such as the well-known antibiotics streptomycin and erythromycin (see Figure 16)(*121*).

Streptomycin   **Erythromycin**
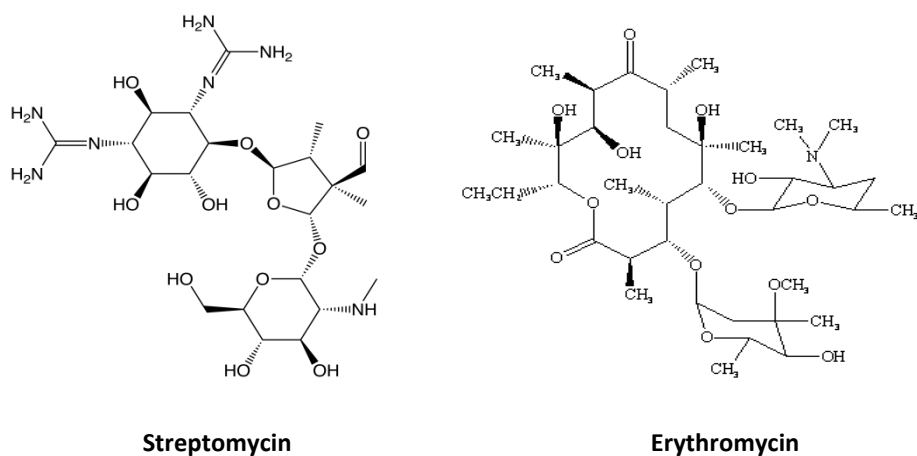
Figure 16. Structures of Streptomycin and Erythromycin, antibiotics isolated from Actinomycete bacteria.

In this project we investigate this class of bacteria again, and screen a library of cave actinomycetes provided by the Bachmann lab for β-hematin inhibition activity using the β-hematin formation assay optimized by the Wright Lab (122). This

actinomycete library has already gone through a pre-screen in the Wright lab, producing

41 active actinomycete extracts to replicate and test in this study. Figure 17 provides an

overview of the discovery and hit identification process. This process is described in

detail in the Experimental section of this chapter.
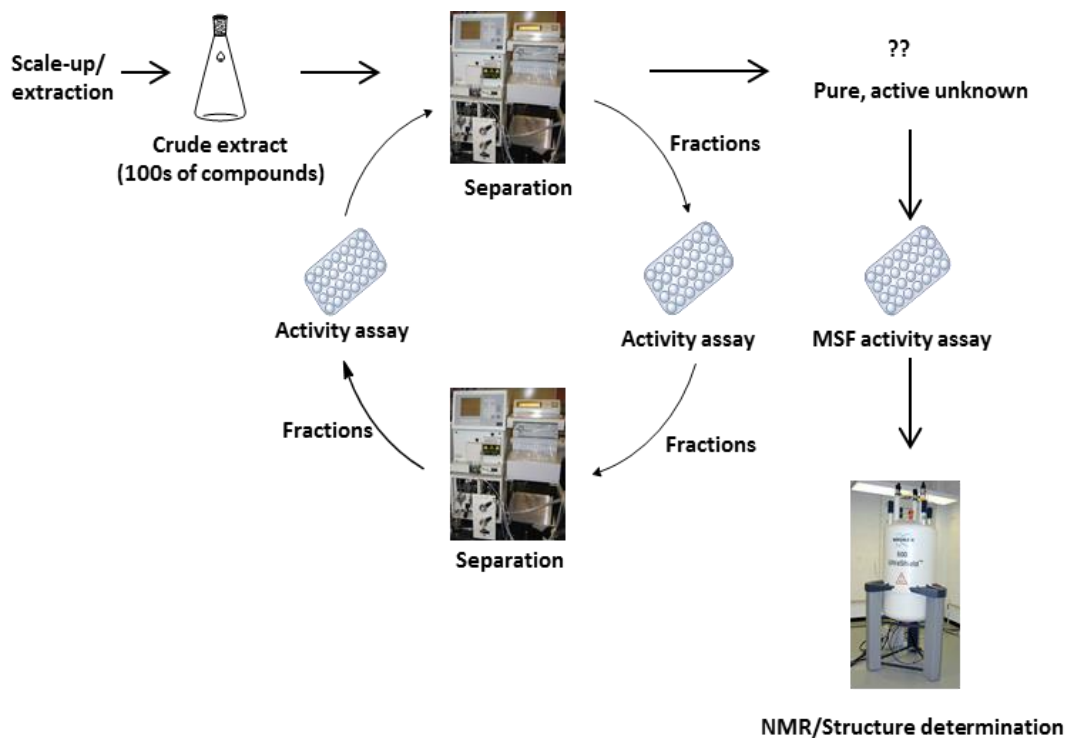
Figure 17. Overview of hit discovery and identification from
Actinomycete strains.

Actinomycetes

Actinomycetes are a species of soil bacteria that have been shown to be

successful producers of bioactive compounds. They are responsible for the production

of nearly half of all discovered bioactive secondary metabolites (*123*). This species has been the source of antibiotics, antitumor agents, and immunosuppressive agents and the subject of intensive study (*123-125*). Recently, success of isolation of novel compounds from terrestrial actinomycetes has declined, and the re-isolation of previously discovered compounds has increased (*126*). Therefore, a need for novel bioactive compounds from actinomycetes is presented. Screening of new actinomycete strains from unexplored or unexploited environments, such as caves, promises to uncover an array of novel bioactive compounds.

<u>Experimental</u>

Growth of Actinomycete Culture

30 μL of an Actinomycete strain were grown on individual solid agar plates for one week at 30°C. Individual colonies were then seeded into six separate flasks containing 50 mL of liquid media, and allowed to incubate at 30°C with shaking for one week. 25mL of 5 of the seed cultures was inoculated into separate 500mL production cultures, and allowed to incubate at 30°C with shaking for one week. This produced 5L of total bacteria culture.

Purification of actinomycete extracts

The 5L of bacterial culture was extracted with an equal amount of solvent, incubated with shaking for 30 minutes, and the resulting mixture spun down at 3500 rpm for 5 minutes. The solvent was removed from the aqueous media, and dried by Rotovap,

producing a crude extract. The crude extract was then purified using both a Sephadex LH-20 column (100% MeOH) and LC-ESI-MS (A: 95% Acetonitrile: 5% H2O, 1mM ammonium Accetate, B: 95% H2O: 5% Acetonitrile, 1mM Ammonium Acetate) to produce two sets of extract fractions. These resulting fractions were transferred to 96-well plates, dried, and screened using the β-hematin formation assay (*122*).

Detergent mediated β-hematin formation assay

The assay conditions were as follows: All liquid delivery was automated using a Thermo Scientific Multidrop Combi robot. To suspend each natural product well fraction, 5-10 μL of acetonitrile was added followed by ten minutes of shaking and 65 μL of water. A 20 μL volume of the hemozoin formation promoter NP-40 (30.55 μM) and 5 μL acetone were added. Finally, a 90 μL volume of hematin (222.2 μM) suspended in 2.0 M sodium acetate solution (pH 4.8) was added to give a final volume of 100 μM hematin. Each plate was incubated at 37C and 55 rpm for at least 5 hours. Upon completion, the assay wells were treated with 25 μL of 50% pyridine solution (pH 7.5) and the plates were shaken for 10 minutes. The absorbance was read at 405 nm using a SpetraMax M5 microplate reader and data was plotted using GraphPad Prism 4. A plate of water and amodiaquine at the IC_{50} was run as negative and positive controls for inhibition. Fractions which showed activity were combined, and put through another round of purification and screening. Rounds of purification and screening were performed until pure fractions containing only active compounds were obtained. The pure compounds were then analyzed by 2D NMR.

2D NMR structure elucidation of Pure Compounds

Active compounds were dissolved in CH_3OD (Sigma Aldrich), and added to a 3mm or 5mm NMR tube. Samples were run using a Bruker AV-II 600 MHz NMR spectrometer. Samples were used for 1D ^{1}H-NMR experiments, as well as 2D NMR suite experiments (COSY, HMBC, HSQC). Data obtained from these experiments will be analyzed, and structures elucidated.

MSF Assay

10mM samples of each active compound will then be tested in an MSF assay following a modified version of the protocol outlined by (113). Briefly, active compounds dissolved in DMSO will be prescreened at 23 μM at a 0.3% starting parasitemia (at 2% hematocrit) in 384-well optical-bottom plates. To establish dose-response curves, active compounds will be delivered in a range of concentrations from 0 to 23 μM with a final DMSO concentration of 0.23% per well. To ensure that DMSO does not interfere with parasite growth, a control plate will be used containing wells with 0.23% DMSO, and wells containing no DMSO will also be used. Concentration-response curves will be generated using GraphPad Prism v5.0

Results

Of the 41 active actinomycete extracts discovered in the preliminary screening, So far, we have been able to reproduce screening data for 5 Actinomycete strains in the Bachmann library (See figure 6). See Appendix A for graphs of all fractions for these

strains. Of the 5 strains for which we were able to reproduce screening data, we found

two compounds that were active both *in vitro* and *in vivo.* The first compound

(Compound A) was found in an actinomycete strain identified as BBHARD25. Compound

A was found to elute at 19.19 minutes using HPLC (A: 95% Acetonitrile: 5% H2O, 1mM

Ammonium Acetate; B: 95% H2O: 5% Acetonitrile, 1mM Ammonium Acetate). Using the

NELI program, we were able to compare HPLC trace with mass and activity data (see

figure 18).
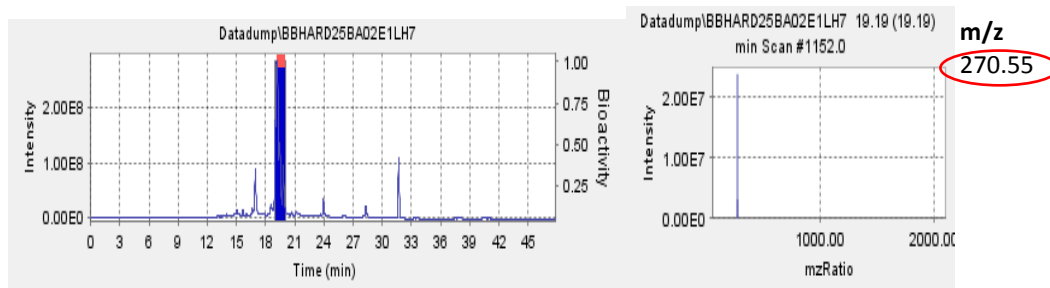
Figure 18. NELI data of BBHARD25 overlapping HPLC data with activity. LC-MS data is
shown on the right.

The NELI data shows an active (highlighted) peak at 19.19 minutes. The LC-MS Mass

data of the peak shows a relatively pure Compound A with an m/z of 270.55. Accurate

mass data of Compound A showed an m/z of 271.06 the difference in m/z

measurements for Compound A are too small to be fragments, and so are most likely

due to differences in MS instrumentation. ^{13}C NMR analysis of Compound A showed the

presence of 1 carbonyl carbon, 12 aromatic carbons, 1 tertiary, and 1 secondary carbon.

A search of the accurate mass and structural components in the Dictionary of Natural

Products database suggested Genistein as a possible identity, while comparison of 2D

NMR data of Compound A with known 2D NMR values of Genistein confirmed the

identity of Compound A as the soy isoflavone Genistein (Table 1, Figure 19).

Table 1. ^{13}C, ^{1}H, and HMBC data for Compound A (600 MHz in CD$_3$O$_3$)

carbon	δ_C	δ_H	HMBC correlations
1	180	C	8, 6
2	104.6	C	4, 6
3	162.9	C	4
4	98.8	CH 6.23 (d)	
5	164.9	C	4, 6
6	93.3	CH 6.35 (d)	
7	158.9	C	8, 6
8	152.9	CH 8.07 (s)	
9	121.8	C	12, 14
10	123.3	C	8, 11, 15
11	130	CH 7.39 (d)	12, 14
12	114.8	CH 6.87 (d)	11, 15
13	157.4	C	11, 12, 14, 15
14	114.8	CH 6.87 (d)	11, 15
15	130	CH 7.39 (d)	12, 14
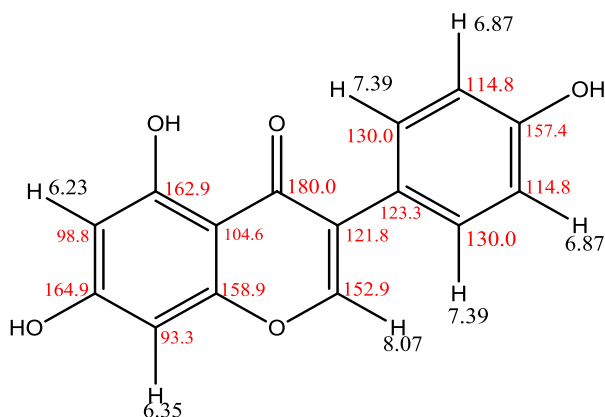
Figure 19. Structure of Genistein with ^{13}C and ^{1}H NMR shifts labeled.

The second compound (Compound B) that was found to be active *in vitro* and *in vivo*

was isolated from an actinomycete strain identified as BBHARD23. Compound B was

found to elute from HPLC at 22.20 minutes HPLC (A: 95% Acetonitrile: 5% H2O, 1mM

Ammonium Acetate; B: 95% H2O: 5% Acetonitrile, 1mM Ammonium Acetate). NELI data

of Compound B shows an active peak at 22.20 minutes. The LC-MS mass data of the

peak shows a major compound with an m/z of 375.75 (See Figure 20), and accurate

mass data of Compound B showed an m/z of 376.13. The small difference in m/z

measurements can be explained by differences in MS instrumentation. Preliminary ^{13}C

NMR data of Compound B suggests the presence of 2 carbonyl carbons, 5 methylene

carbons, 8 methnine carbons, and 10 quaternary carbons. A full 2D NMR analysis of

Carbon B is in progress.

Figure 20. NELI data of BBHARD23 overlapping HPLC data with activity. LC-MS data is shown on the right.

Conclusion

We were able to reproduce results from the initial screening, and found that the Bachmann lab Actinomycete library produced many active fractions. Two fractions that were active in the β-hematin assay were purified to produce two active compounds. One of these compounds (Compound A) was identified by MS data and 2D NMR as the soy isoflavone Genistein. It is most likely that Genistein was obtained as a media component, instead of a product of Actinomycete metabolism, since Actinomycete growth media used in this study routinely contained ground soybeans. Structure determination of Compound B by MS and 2D NMR is in progress.

Chapter III

Anti-malarial Effects of Genistein

<u>Introduction</u>

Genistein is an isoflavonoid commonly found in soybeans. It is the simplest of the isoflavanoid compounds, and an important precursor to more complex isoflavanoids that have antimicrobial action (127). Studies on Genistein show it to have tyrosine kinase activity, and action against cancer and cardiovascular disease (127). Genistein has also been found to be active against liver and blood stage malaria parasite, reducing liver infections by 64% in mice given Genistein 6hrs prior to infection, and blood infections by 33% when administered at 200uM (128, 129).The antimalarial activity of genistein in these studies was attributed to its function as a tyrosine kinase inhibitor, but no link to any interaction with hemozoin has been found. In this study, we found the active component of an actinomycete extract to be genistein.

<u>Experimental</u>

Growth of Actinomycete Culture

30 μL of an Actinomycete strain were grown on individual solid agar plates for one week at 30°C. Individual colonies were then seeded into six separate flasks containing 50 mL

of liquid media, and allowed to incubate at 30°C with shaking for one week. 25mL of 5 of the seed cultures was inoculated into separate 500mL production cultures, and allowed to incubate at 30°C with shaking for one week. This produced 5L of total bacteria culture.

Purification of actinomycete extracts

The 5L of bacterial culture was extracted with an equal amount of ethylacetate,, incubated with shaking for 30 minutes, and the resulting mixture spun down at 3500 rpm for 5 minutes. The solvent was removed from the aqueous media, and dried by Rotovap, producing a crude extract. The crude extract was then purified using both a Sephadex LH-20 column (100% MeOH) and LC-ESI-MS (A: 95% Acetonitrile:5% H_2O, B: 5% Acetonitrile: 95% H_2O, 1mM Ammonium Acetate) to produce two sets of extract fractions. These resulting fractions were transferred to 96-well plates, dried, and screened using the β-hematin formation assay (*46*).

Detergent mediated B-hematin formation assay

The assay conditions were as follows: All liquid delivery was automated using a Thermo Scientific Multidrop Combi robot. To suspend each natural product well fraction, 5-10 μL of acetonitrile was added followed by ten minutes of shaking and 65 μL of water. A 20 μL volume of the hemozoin formation promoter NP-40 (30.55 μM) and 5 μL acetone were added. Finally, a 90 μL volume of hematin (222.2 μM) suspended in 2.0 M sodium acetate solution (pH 4.8) was added to give a final volume of 100 μM hematin. Each plate was incubated at 37°C and 55 rpm for at least 5 hours. Upon completion, the assay

wells were treated with 25 µL of 50% pyridine solution (pH 7.5) and the plates were

shaken for 10 minutes. The absorbance was read at 405 nm using a SpetraMax M5

microplate reader and data was plotted using GraphPad Prism 4. A plate of water and

amodiaquine at the IC_{50} was run as negative and positive controls for inhibition.

Fractions which showed activity were combined, and put through another round of

purification and screening. Rounds of purification and screening were performed until

pure fractions containing only active compounds were obtained. The pure compounds

were then analyzed by 2D NMR.

2D NMR structure elucidation of Pure Compounds

Active compounds were dissolved in CH_3OD (Sigma Aldrich), and added to a 3mm or

5mm NMR tube. Samples were run using a Bruker AV-II 600 MHz NMR spectrometer.

Samples were used for ^{1}H-NMR experiments, as well as 2D NMR suite experiments

(COSY, HMBC, HSQC). Data obtained from these experiments will be analyzed, and

structures elucidated.

MSF Assay

10mM samples of each active compound will then be tested in an MSF assay following a

modified version of the protocol outlined by (*113*). Briefly, active compounds dissolved

in DMSO will be prescreened at 23 µM at a 0.3% starting parasitemia (at 2% hematocrit)

in 384-well optical-bottom plates. To establish dose-response curves, active compounds

will be delivered in a range of concentrations from 0 to 23 µM with a final DMSO

concentration of 0.23% per well. To ensure that DMSO does not interfere with parasite

growth, a control plate will be used containing wells with 0.23% DMSO, and wells containing no DMSO will also be used. Concentration-response curves will be generated using GraphPad Prism v5.0

Results

MSF assays of the Genistein isolated from BBHARD25 and the isolated active fraction from BBHARD23 showed very little activity. The IC_{50} values of these fractions were 18μM, an order of magnitude less active than chloroquine (See figure 21). To confirm that Genistein is the active compound, a β-hematin assay was performed on synthetic Genistein. The IC_{50} curves of the β-hematin assay performed on synthetic Genistein showed no activity (See figure 22). Therefore, it is likely that Genistein was not the major contributor of activity in the β-hematin assay from BBHARD25. Further analysis of NELI data shows the presence of another compound at very low levels (See Figure 23). LC-MS data shows that the second compound has an m/z of 412.72. Efforts to obtain NMR and accurate mass data from this compound were unsuccessful due to the limited amount of sample that was left, and the low concentration of the compound.
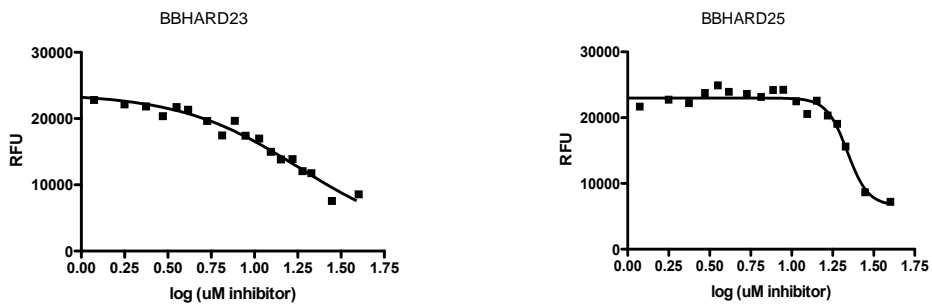
Figure 21: MSF assay IC$_{50}$ curves of active fractions from BBHARD23 and BBHARD25
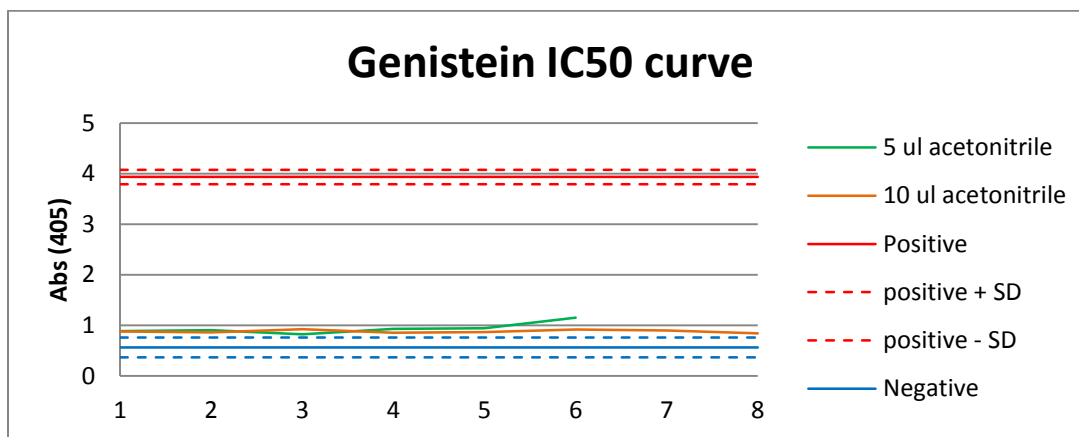
Figure 22: IC$_{50}$ curve of synthetic genistein performed under normal assay conditions.
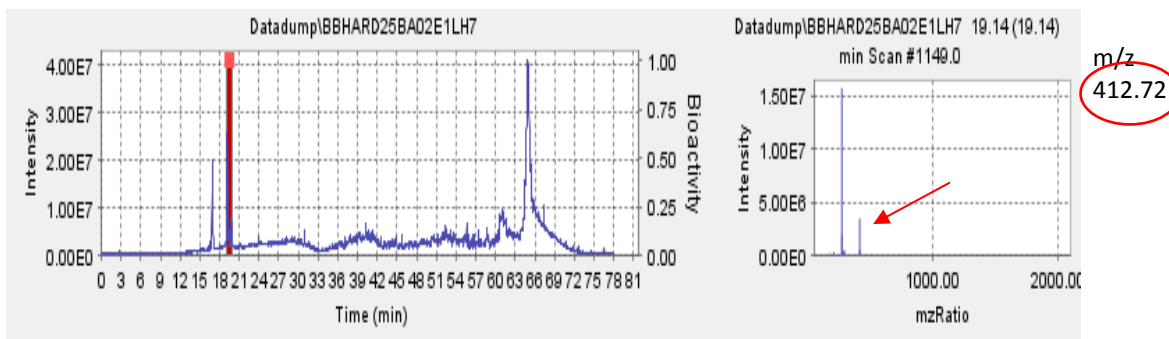
Figure 23. NELI data of BBHARD25 overlapping HPLC data with activity. LC-MS data is shown on the right, revealing the presence of a second compound with m/z of 412.72.

Conclusion

Although the isolated genistein did not show high levels of activity *in vivo,* it is promising that activity can be seen in the malaria parasite even at low levels. Using SAR studies, it may be possible to modify the active scaffolds to increase antimalarial activity, thereby producing a novel antimalarial treatment. Since synthetic Genistein showed no activity in vitro, this suggests that another compound was responsible for that activity. The second compound found in the active fraction at low levels it is also possible that another compound present at very low levels is causing the anti-malarial activity in the β-hematin assay. This is interesting because any compound producing anti-malarial activity at such low levels is probably very potent. Efforts to obtain NMR and accurate mass data from this unknown compound were unsuccessful due to the limited amount and low concentration of the sample. A more concentrated sample may be obtained by growing another culture of the BBHARD25 actinomycete strain, and re-isolating the unknown compound.

β-HEMATIN ASSAYS OF ACTINOMYCETE STRAINS

BBELLIUNKA01 LH6

BBELLIUNKA01 LH7

BBELLIUNKA01 LH8

BBHARD19 Crude Extract

BBHARD19 LH2
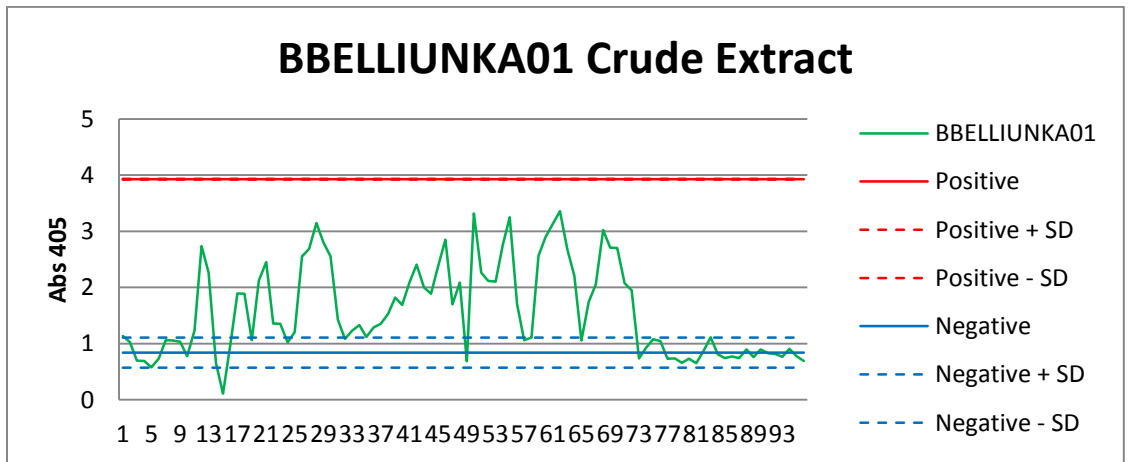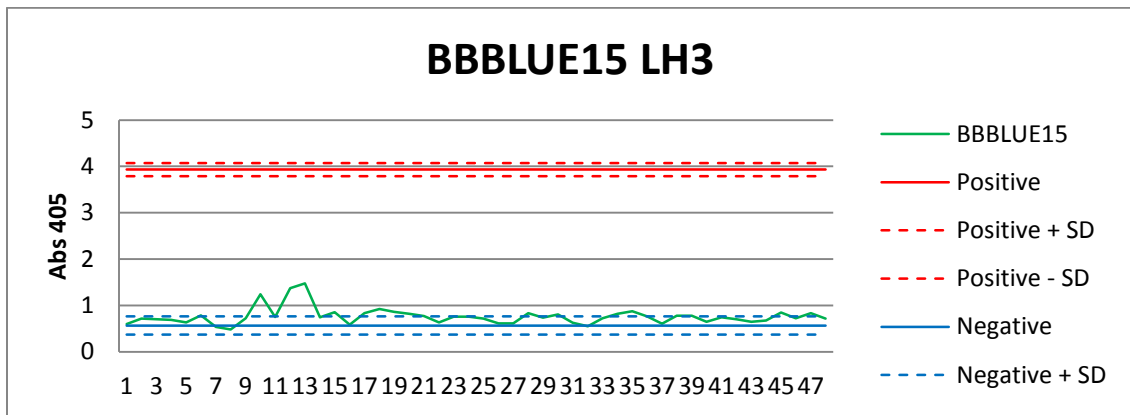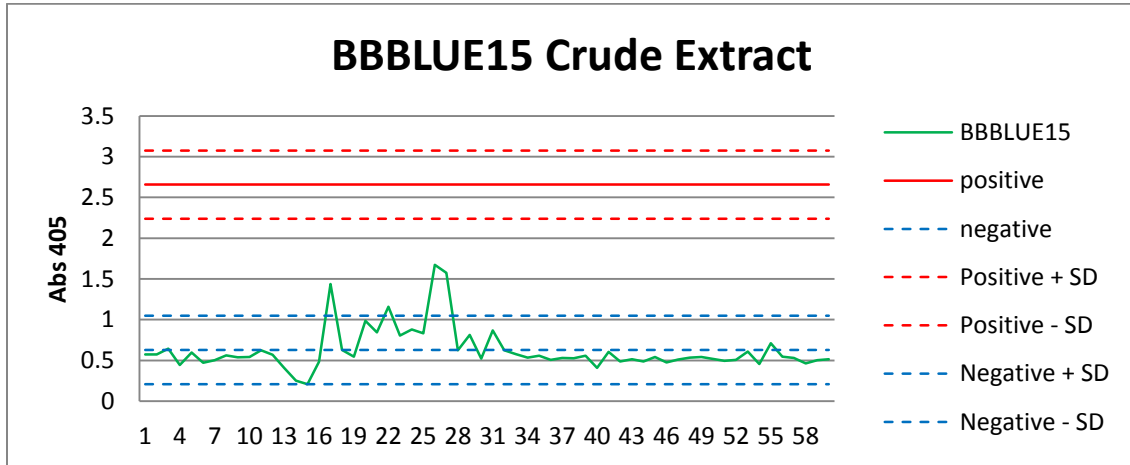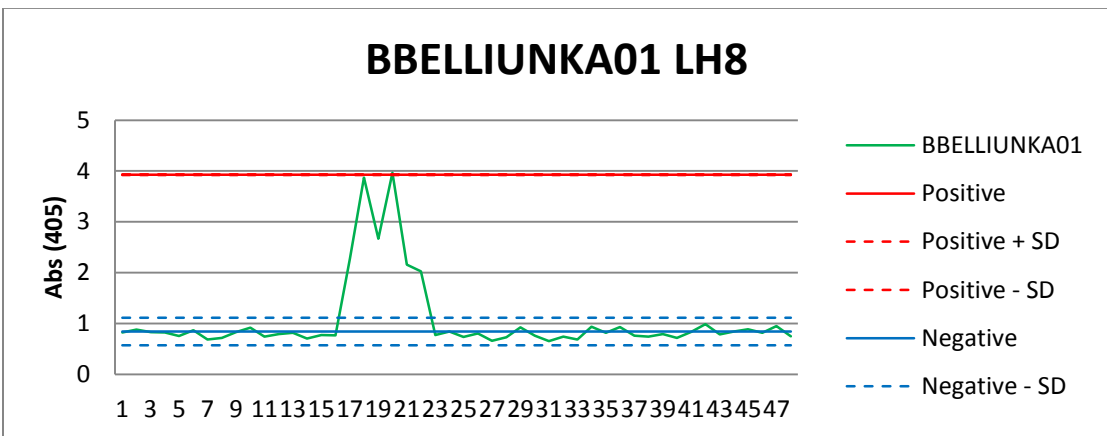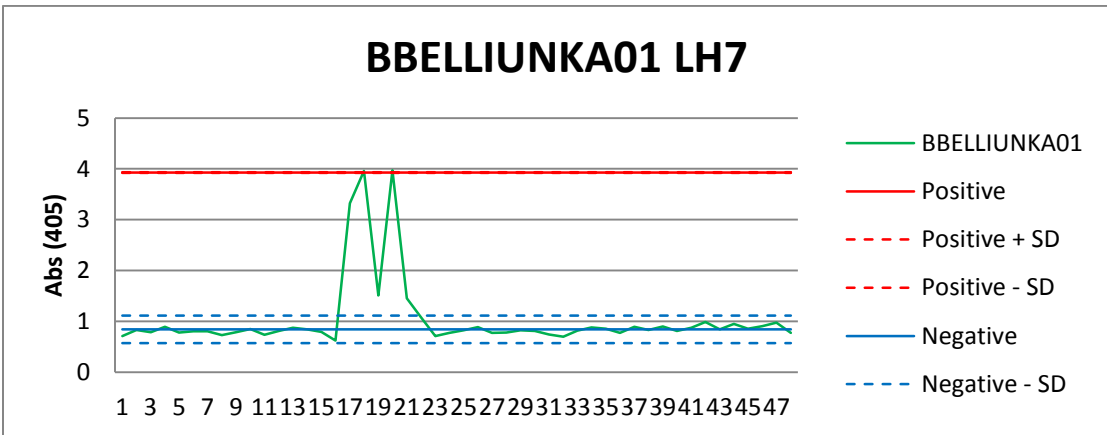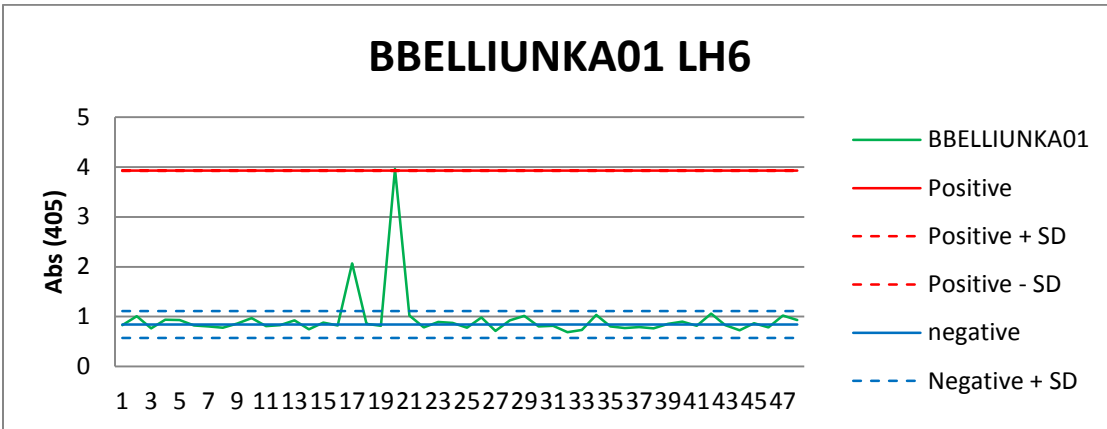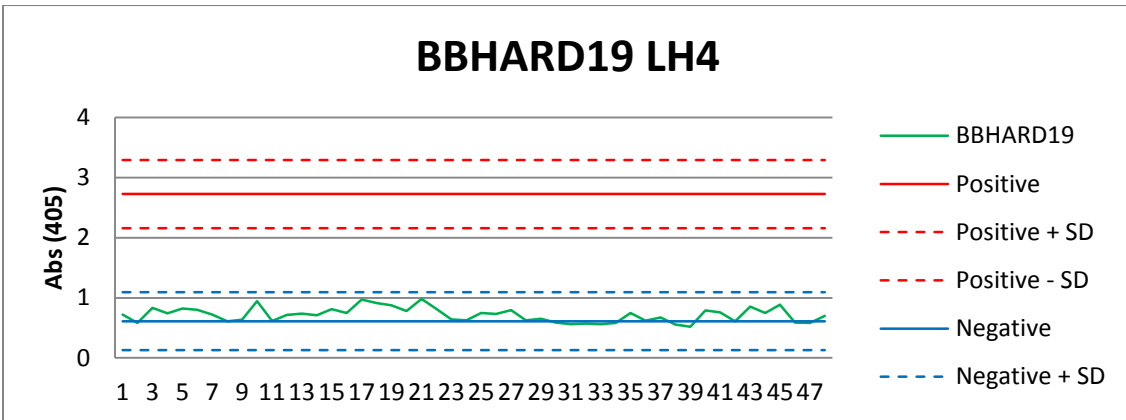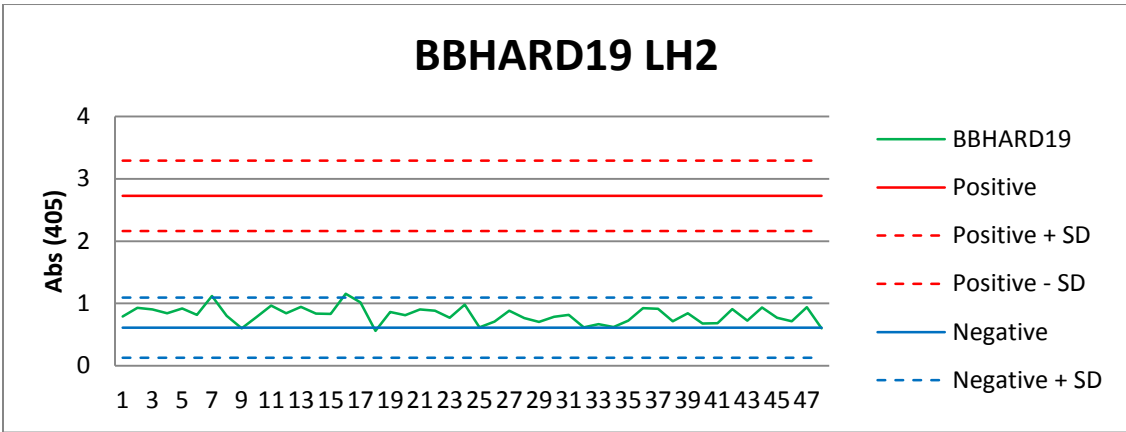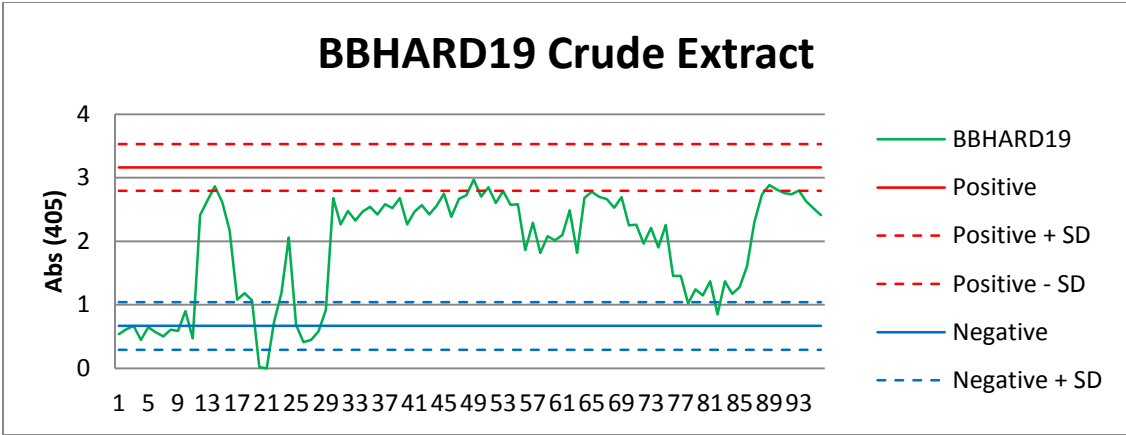
BBHARD19 LH4
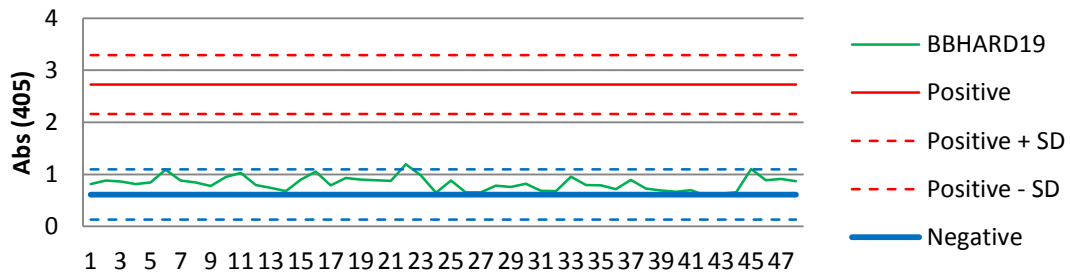
BBHARD19 LH6
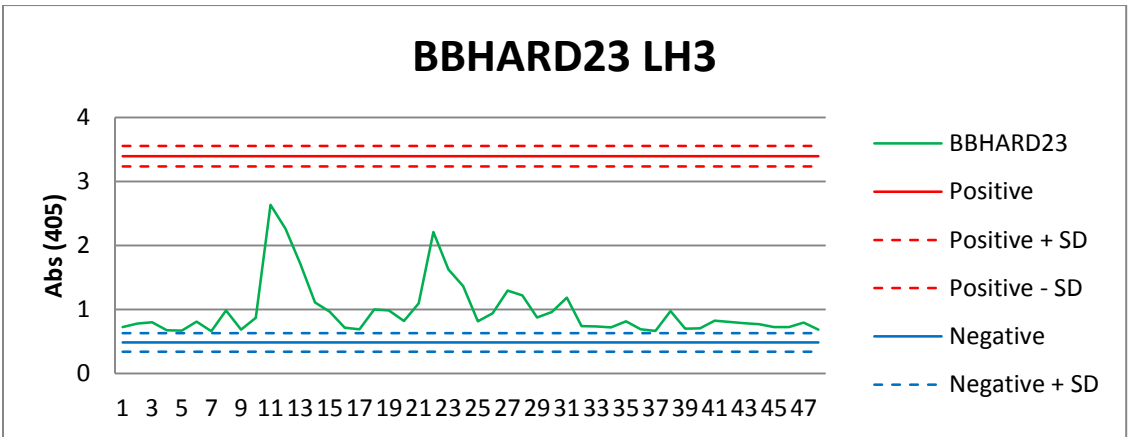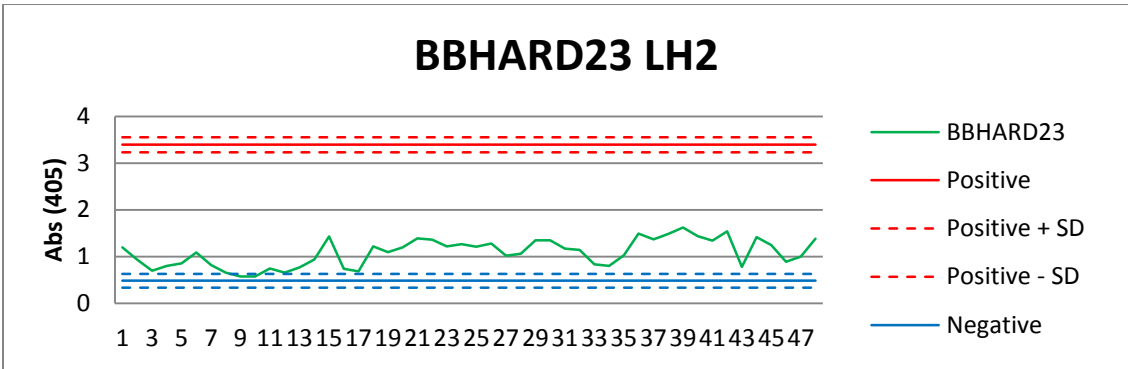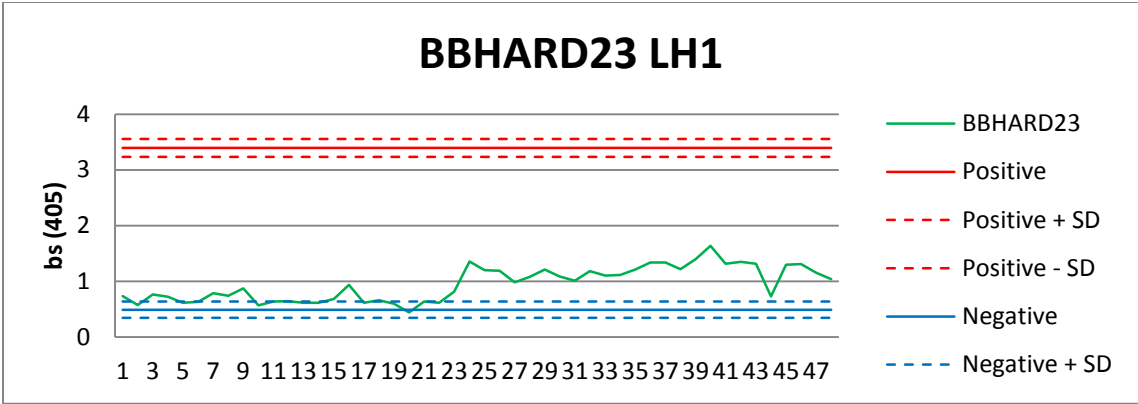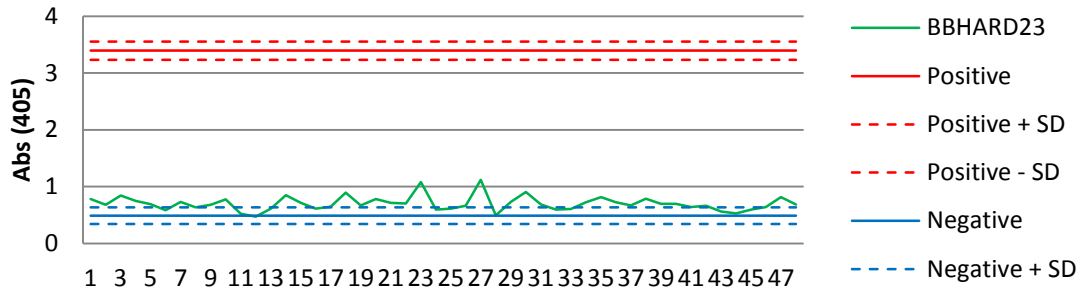
BBHARD19 LH8
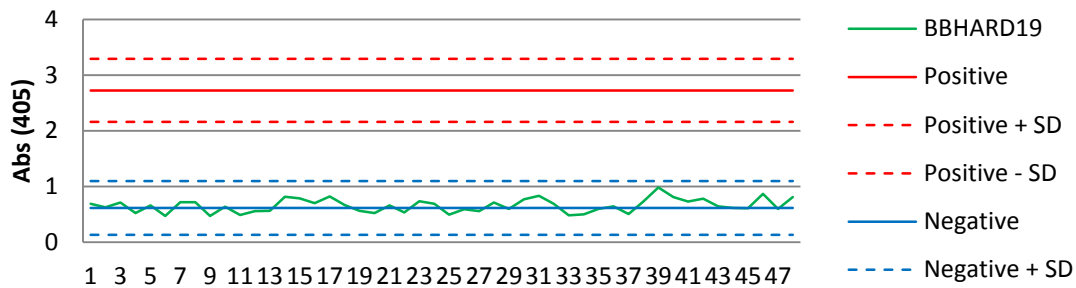
BBHARD23 Crude Extract

BBHARD23 LH1
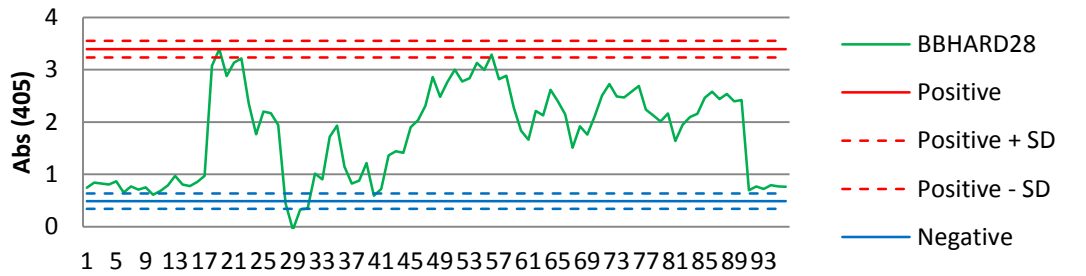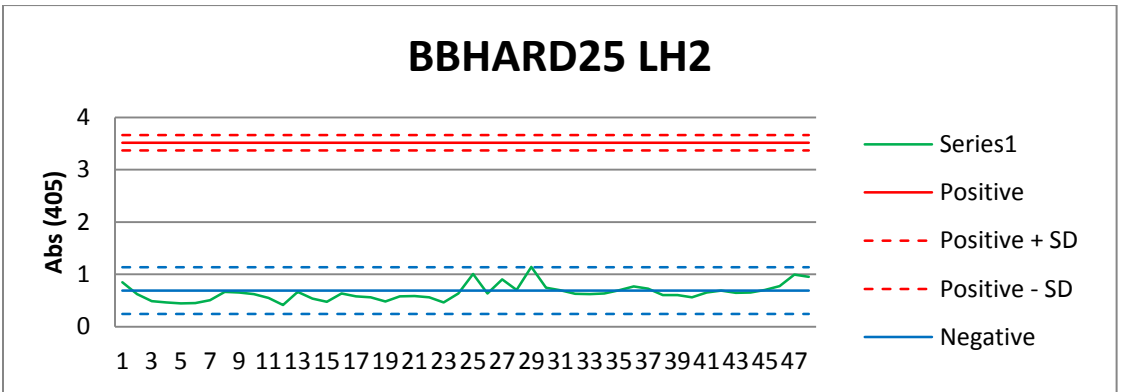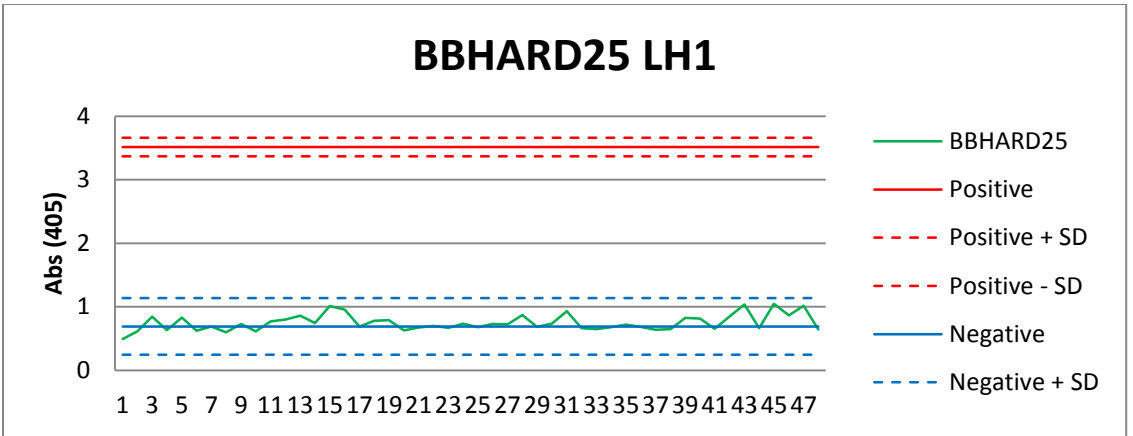

BBHARD23 LH2

BBHARD23 LH3

64
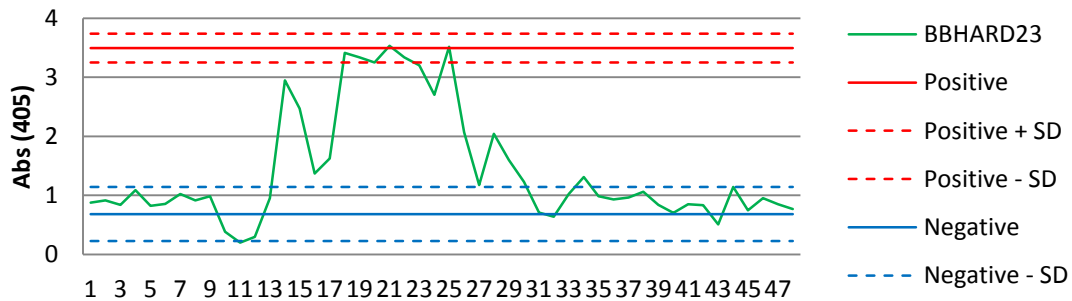
BBHARD23 LH4

BBHARD23 LH5
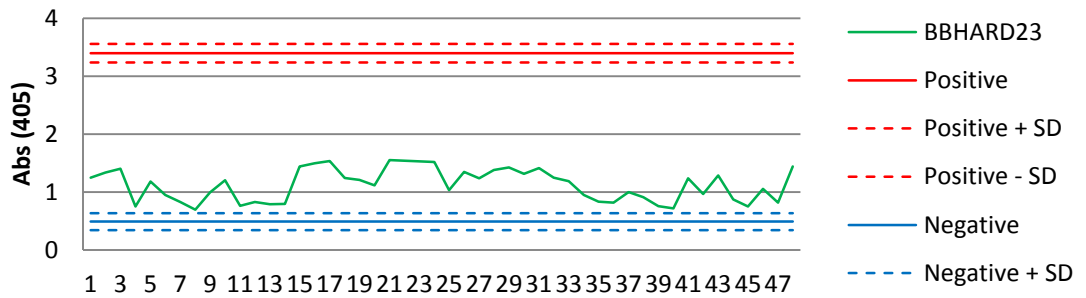
BBHARD28 Crude Extract

BBHARD25 Crude Extract

BBHARD25 LH1
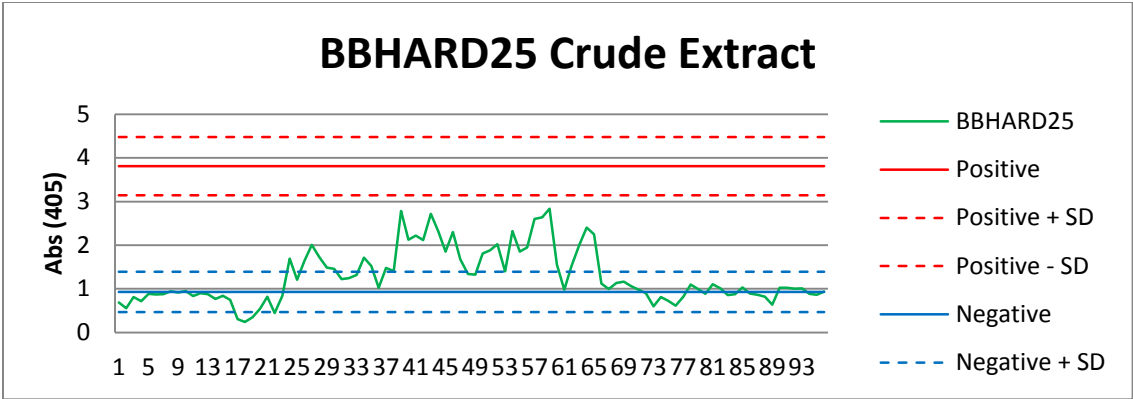
BBHARD25 LH2
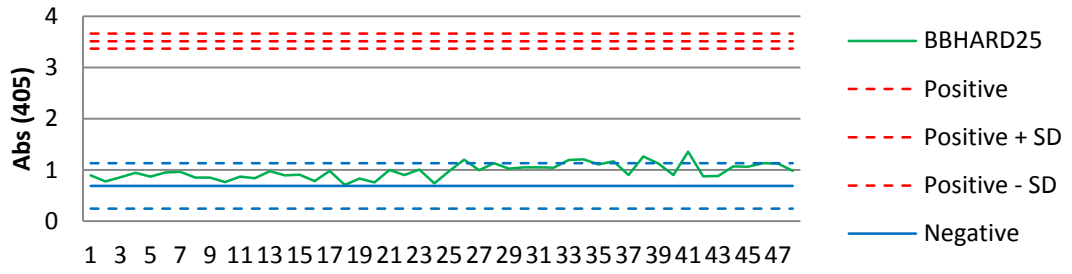
BBHARD25 LH3
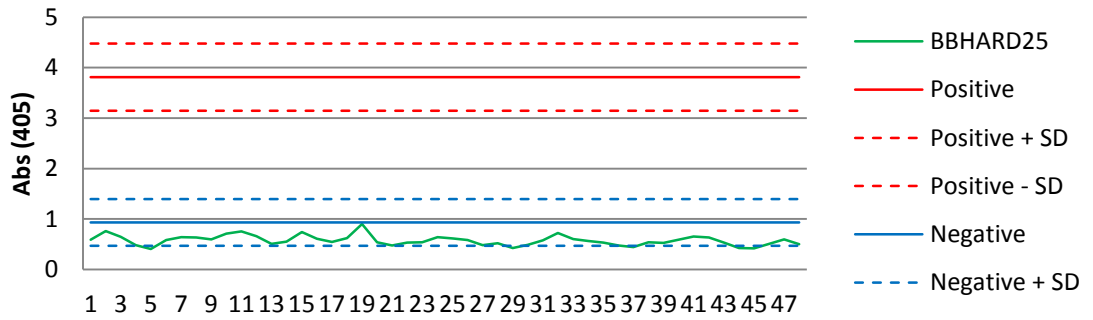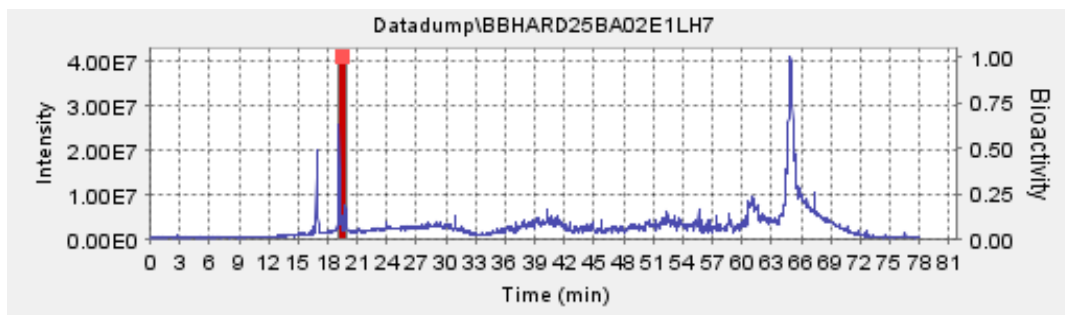

BBHARD25 LH4
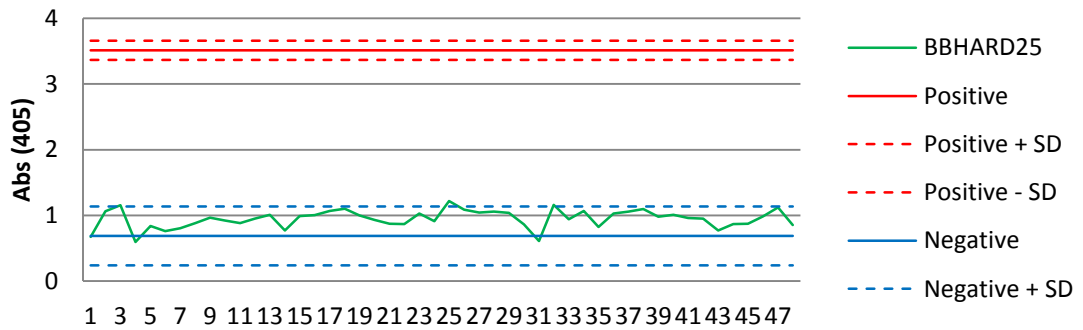
BBHARD25 LH5
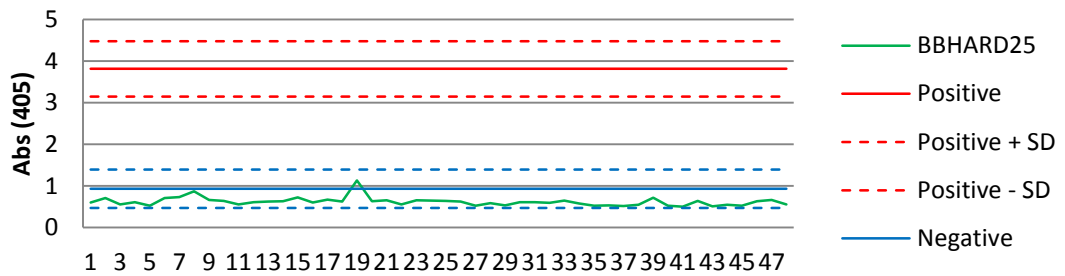
BBHARD25 LH6
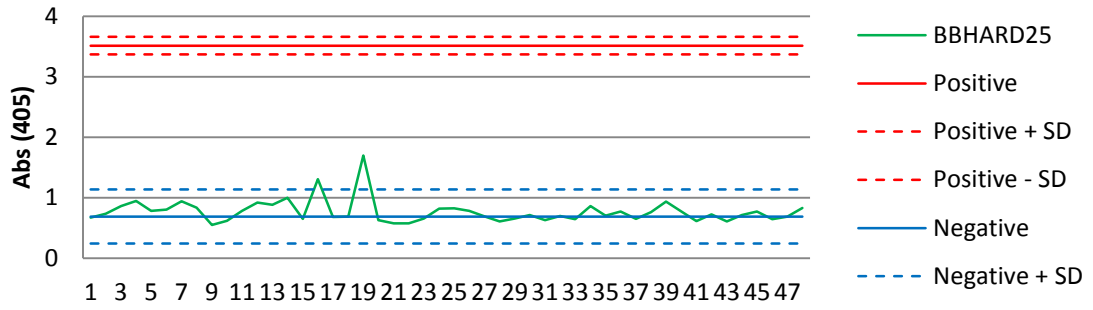
BBHARD25 LH7

APPENDIX B

CHROMOTOGRAPHY PROFILES OF ACTIVE COMPOUNDS

NELI data of BBHARD25 HPLC trace overlapped with activity data.
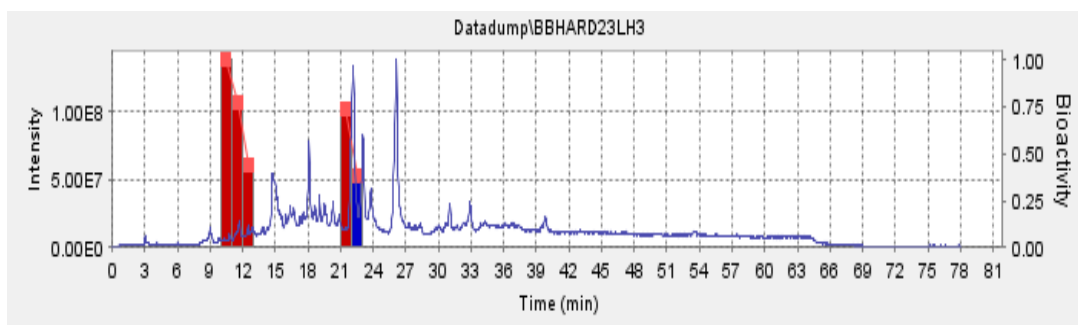
NELI data of BBHARD23 HPLC trace overlapped with activity data.

MASS ANALYSIS DATA OF BBHARD 25 AND BBHARD23

Mass analysis data of active component of BBHARD25

Elemental Composition Report

Page 1

Single Mass Analysis
Tolerance = 5.0 PPM / DBE: min = -1.5, max = 50.0
Element prediction: Off
Number of isotope peaks used for i-FIT = 3

Monoisotopic Mass, Even Electron Ions
45289 formula(e) evaluated with 64 results within limits (up to 50 best isotopic matches for each mass)
Elements Used:
C: 1-100 H: 1-50 N: 0-10 O: 0-20 Na: 0-2 P: 0-5 S: 0-5 K: 0-2

Sample Cone Voltage = 30
Coll Energy = 6

120706_MWC_Carroll_BBH23_PosV_EDR_FullScan 278 (5.371) Cm (270:278)

1: TOF MS ES+
1.85e+004
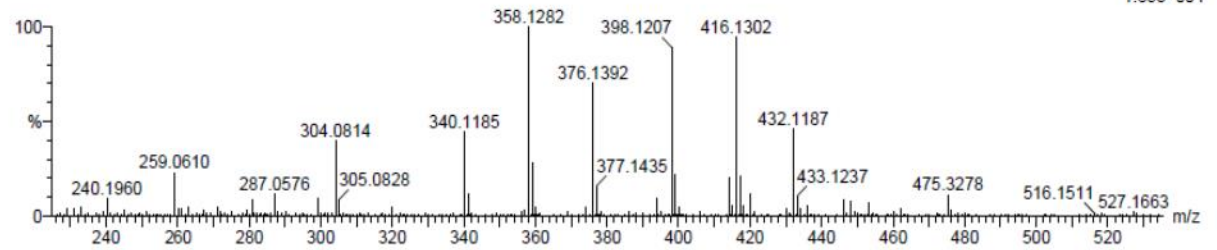
| Minimum: | | | -1.5 | |
| Maximum: | 100.0 | 5.0 | 50.0 | |

Mass analysis data of active fraction from BBHARD23
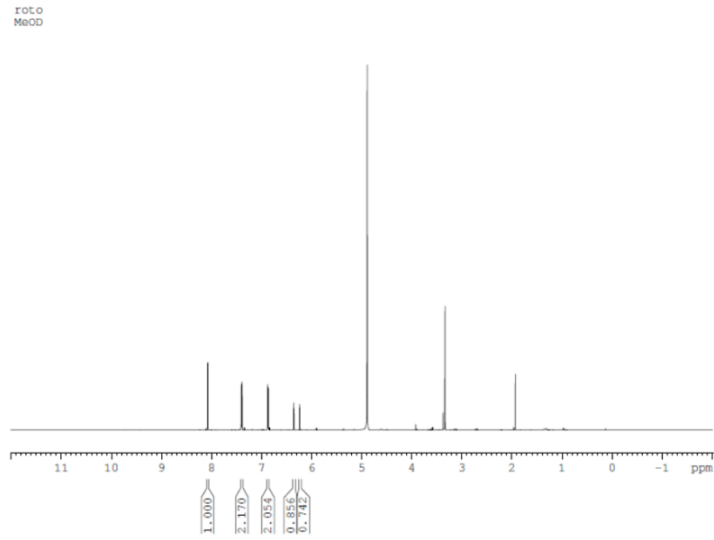
^{1}H NMR data of active component of BBHARD25
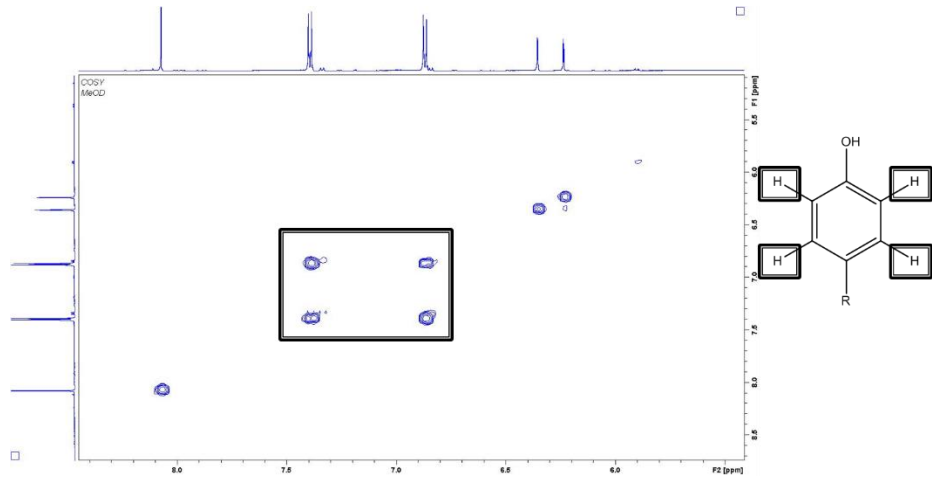
COSY NMR data of active component of BBHARD25
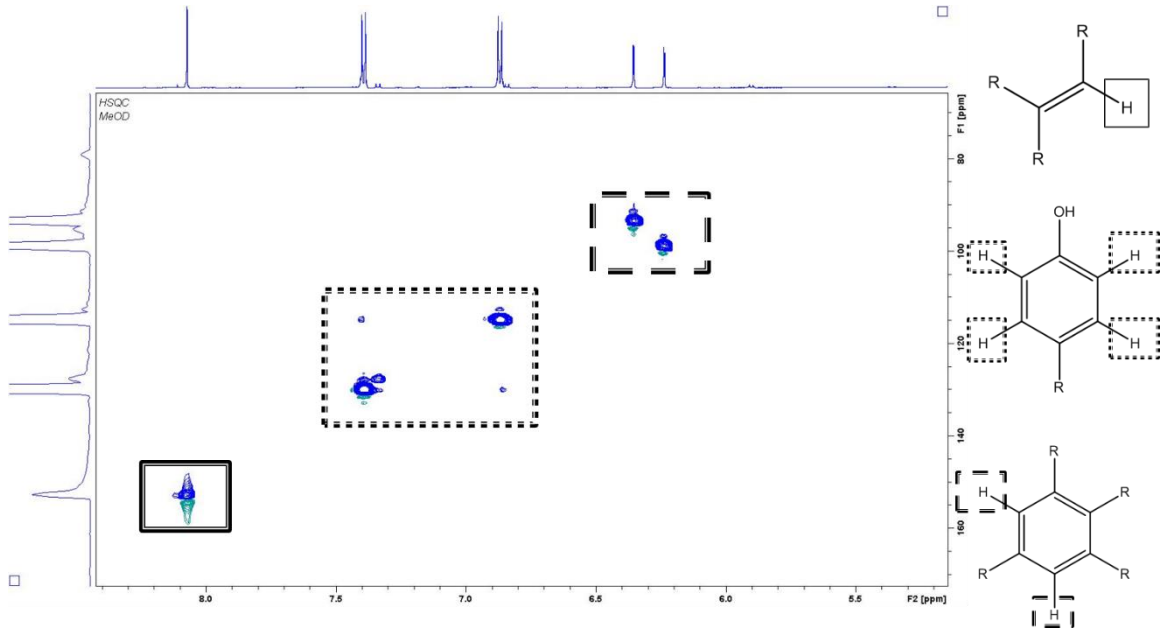
HSQC NMR data of active component of BBHARD25
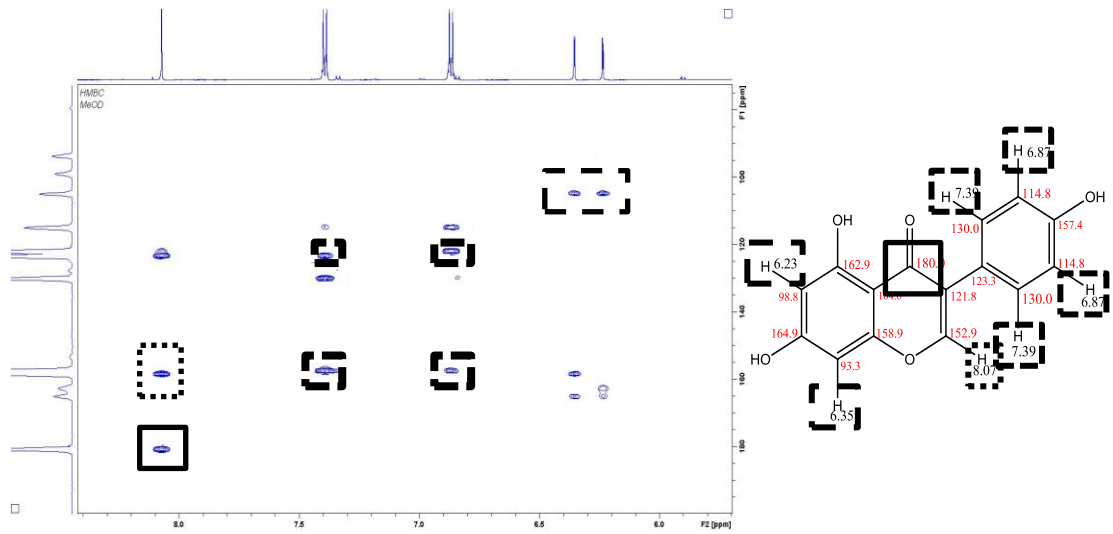
HMBC NMR data of active component of BBHARD25

CURRICULUM VITAE

HOLLY MARIE CARRELL

EDUCATION

Vanderbilt University, Nashville, TN

M.S. in Chemistry   **2013**

   Thesis: "Isolation and Characterization of Anti-malarial Compounds From a Natural Product Library"

Oakwood University, Huntsville, AL

B.S. in Biochemistry   **2009**

AWARDS

Provost's Graduate Fellowship, Vanderbilt University   **2009 – Present**
Premier Scholarship, Oakwood University   **2005 – 2009**

TEACHING EXPERIENCE

Vanderbilt University, Nashville, TN

Teaching Assistant – to Professor Adam List in "Organic Chemistry Lab"   **2010-2012**
Supervised lab experiments, held office hours, administered quizzes and lab final, documented all grades.

Oakwood University, Huntsville, AL

Teaching Assistant – to Professor Kenneth LaiHing in "Organic Chemistry Lab"   **2008**
Supervised lab experiments, administered quizzes and lab final, documented all grades.

Teaching Assistant – to Professor Kenneth LaiHing in "General Chemistry Lab"   **2006-2007**
Supervised lab experiments, administered quizzes and lab final, documented all grades.

RELATED EXPERIENCE

Vanderbilt University, Nashville, TN

Graduate Research assistant – to Professor David Wright   **2009 – 2012**

Experiment design and execution, data collection and analysis on isolating and identifying antimalarial probes from a natural product library.

Oakwood University, Huntsville, AL
Research Assistant – to Professor Alexander Volkov   **2007 – 2009**
Design and execute experiments on the electrophysiology of the Venus Flytrap, data collection and analysis.

Oakwood University, Huntsville, AL
Research Assistant – to Professor Christopher Perry   **2006-2008**
Responsible for data collection by Atomic Force Microscopy on various projects.

Donald Danforth Plant Science Center, St. Louis, MO
Research Intern   **2007**
Conducted research on the mode of action of plant defensins in the inhibition of *Fusarium graminearum*.

PUBLICATIONS AND PAPERS

Sandlin, Rebecca D., Holly M. Carrell, and David W. Wright. "Hemozoin: Crystal Engineering Survivability." *Encyclopedia of Inorganic and Bioinorganic Chemistry*.

Volkov, Alexander G., Holly Carrell, and Vladislav S. Markin. "Biologically closed electrical circuits in Venus flytrap." *Plant Physiology* 149.4 (2009): 1661-1667.

Volkov, Alexander G., et al. "Electrical memory in Venus flytrap."*Bioelectrochemistry* 75.2 (2009): 142-147.

Volkov, Alexander G., Holly Carrell, and Vladislav S. Markin. "Molecular electronics of the Dionaea muscipula trap." *Plant signaling & behavior* 4.4 (2009): 353-354.

Volkov, Alexander G., et al. "Plant electrical memory." *Plant signaling & behavior* 3.7 (2008): 490-492.

Waddell, Emanuel A., et al. "Surface modification of Sylgard 184 polydimethylsiloxane by 254nm excimer radiation and characterization by contact angle goniometry, infrared spectroscopy, atomic force and scanning electron microscopy." *Applied Surface Science* 254.17 (2008): 5314-5318.

REFERENCES

1. Perutz, M. F., *Sci. Am.* **1978**, *239* (6), 92.

2. Wittenberg, B.; Wittenberg, J., *Annu. Rev. Physiol.* **1989**, *51* (1), 857.

3. Mason, H., *Science.* **1957**, *125* (3259), 1185.

4. Gong, W.; Hao, B.; Mansy, S. S.; Gonzalez, G.; Gilles-Gonzalez, M. A., Chan, M. K., *Proc. Natl. Acad. Sci.* **1988**, *95* (26), 15177.

5. Nath, K. A.; Balla, J.; Croatt, A. J.; Vercellotti, G. M., *Kidney Int.* **1995**, *47* (2), 592.

6. Nath, K.A., Vercellotti, G.M., Grande, J.P., Miyoshi, H., Paya, C.V., Manivel, J.C., Haggard, J.J., Croatt, A.J., Payne W.D., Alam, J., *Kidney Int.* **2001**, 59 (1), 106.

7. Aft, R., Mueller, G., *J. Biol. Chem.* **1984**, 259 (1), 301.

8. Miller, Y. I., Shaklai, N., *Biochem. Mol. Biol. Int.* **1994**, 34 (6), 1121. Epub 1994/12/01.

9. Suliman, H. B., Carraway, M. S., Velsor, L. W., Day, B. J., Ghio, A. J., Piantadosi, C. A., *Free Radical Biol. Med.* **2002**, 32 (3), 246.

10. Castellani, R., Harris, P., Lecroisey, A., Izadi-Pruneyre, N., Wandersman, C., Perry, G., Smith, M. A., *Antioxid. Redox Signaling*. **2000**, 2 (1), 137.

11. Kutty, R., Daniel, R. F., Ryan, D. E., Levin W., Maines, M. D., *Arch. Biochem. Biophys.* **1988**, 260 (2), 638.

12. Docherty, J.C., Firneisz, G.D., Schacter, B.A., *Arch. Biochem. Biophys.* **1984**, 235 (2), 657.

13. Ryter, S.W., Tyrrell, R.M., *Free Radical Biol. Med.* **2000**, 28 (2), 289.

14. Tenhunen, R., Marver, H.S., Schmid, R., *J. Biol. Chem.* **1969**, 244, 6388.

15. Francis, S.E., Sullivan, D.J., Goldberg, D.E., *Annu. Rev. Microbiol.* **1997**, 51 (1), 97.

16. Morrison, D.B., Jeskey, H.A., *J. Natl. Malar. Soc.* **1948**, 7 (4), 259. Epub 1948/12/01.

17. Ball, E., McKee, R., Anfinsen, C., Cruz, W., Geiman, Q., *J. Biol. Chem.* **1948**, 175 (2), 547.

18. Orjih, A.U., Fitch, C.D., *Biochim. Biophys. Acta*. **1993**, 1157 (2), 270.

19. Sherman, I., *Bull. World Health Organiz.* **1977**, 55 (2–3), 265.

20. Ting, I.P., Sherman, I.W., *Comp. Biochem. Physiol.* **1966**, 19 (4), 855.

21. Alan, F. C., Brendan, S. C., *Cell*. **2006**, 124, 755.

22. Sherman I.W., Tanigoshi, L., *Int. J. Biochem.* **1970**, 1 (5), 635.

23. Theakston, R.D., Fletcher, K.A., Maegraith, B.G., *Ann. Trop. Med. Parasitol.* **1970**, 64 (1), 63. Epub 1970/03/01.

24. McCormick, G.J., *Exp. Parasitol.* **1970**, 27 (1), 143.

25. Slomianny, C., *Blood Cells*. **1990**, 16 (2–3), 369. Epub 1990/01/01.

26. Olliaro, P., Goldberg, D., *Parasitol. Today*. **1995**, 11 (8), 294.

27. Goldberg, D., Slater, A., Cerami, A., Henderson, G., *Proc. Natl. Acad. Sci. U. S. A.*, **1990**, 87 (8), 2931.

28. Francis, S.E., Gluzman, I.Y., Oksman, A., Banerjee, D., Goldberg, D.E., *Mol. Biochem. Parasitol.* **1996**, 83 (2), 189.

29. Gluzman, I.Y., Francis, S.E., Oksman, A., Smith, C.E., Duffin, K.L., Goldberg, D.E., *J. Clin. Invest.* **1994**, 93 (4), 1602.

30. Kolakovich, K.A., Gluzman, I.Y., Duffin K. L., Goldberg, D. E., *Mol. Biochem. Parasitol.* **1997**, 87 (2), 123.

31. Coombs, G., Goldberg, D., Klemba, M., Berry, C., Kay, J., Mottram, J., *Trends Parasitol.* **2001**, 17 (11), 532.

32. Berry, C., Humphreys, M., Matharu, P., Granger, R., Horrocks. P., Moon, R., Certa, U., Ridley, R.G., Bur, D., Kay, J., *FEBS Lett.* **1999**, 447 (2–3), 149.

33. Goldberg, D., Slater, A., Beavis, R., Chait, B., Cerami, A., Henderson, G., *J. Exp. Med.* **1991**, 173 (4), 961.

34. Banerjee, R., Liu, J., Beatty, W., Pelosof, L., Klemba, M., Goldberg, D. E., *Proc. Natl. Acad. Sci.* **2002**, 99 (2), 990.

35. M. F. Perutz, M.F., Edited by Stamatoyannopoulos, G., Nienhuis. A.W., Saunders, W.B., Philadelphia, **1987,** 127.

36. Wyatt, D.M., Berry, C., *FEBS Lett.* **2002**, 513 (2–3), 159.

37. Rosenthal, P.J., Nelson, R.G., *Mol. Biochem. Parasitol.* **1992**, 51 (1), 143.

38. Sijwali, P.S., Shenai, B.R., Gut, J., Singh, A., Rosenthal, P.J., *Biochem. J.* **2001**, 360 (2), 481.

39. Shenai, B.R., Sijwali, P.S., Singh, A., Rosenthal, P.J., *J. Biol. Chem.* **2000**, 275 29000.

40. Shenai, B.R., Rosenthal, P.J., *Mol. Biochem. Parasitol.* **2002**, 122 (1), 99.

41. Eggleson, K.K., Duffin, K.L., Goldberg, D.E., *J. Biol. Chem.* **1999**, 274, 32411.

42. Gluzman, I.Y., Francis, S.E., Oksman, A., Smith, C.E., Duffin, K.L., Goldberg, D.E., *J. Clin. Invest*. **1994**, 93 (4), 1602.

43. Fitch, C., Chevli, R., Kanjananggulpan, P., Dutta, P., Chevli, K., Chou, A., *Blood*. **1983**, 62 (6), 1165.

44. Becker, K., Tilley, L., Vennerstrom, J.L., Roberts, D., Rogerson, S., Ginsburg, H., *Int. J. Parasitol.* **2004**, 34 (2), 163.

45. Har-el, R., Marva, M., Chevion, M., Golenser, J., *Free Radical Res.* **1993**, 18 (5), 279.

46. Lancisi, G.M., in 'De Noxiis Paludum Effluvius Eorumque Remediis', ed. Salvioni, J. M., Rome, **1717**.

47. Golgi, C., Representation photographique du development des parasites de l'infection paldeene, Verhandldes X Internat. Med. Cong. Berlin Bd II abth III.200, 1890.

48. Weissbuch, I., Leiserowitz, L., *Chem. Rev.* **2008**, 108, 4899.

49. Chen, M.M., Shi, L., Sullivan Jr, D.J., *Mol. Biochem. Parasitol.* **2001**, 113, 1.

50. Noland, G.S., Briones, N., Sullivan Jr, D.J., *Mol. Biochem. Parasitol.* **2003**, 130, 91.

51. Pagola, S., Stephens, P.W., Bohle, D.S., Kosar, A.D., Madsen, S.K., *Nature* **2000**, 404 (6775), 307.

52. Pasternack, R.F., Munda, B., Bickford, A., Gibbs, E.J., Scolaro, L.M., *J. Inorg. Biochem.* **2010**, 104 (10), 1119. Epub 2010/07/30.

53. Klonis, N., Dilanian, R., Hanssen, E., Darmanin, C., Streltsov, V., Deed, S., Quiney, H., Tilley, L., *Biochemistry* **2010**, 49 (31), 6804.

54. Slater, A.F., Swiggard, W.J., Orton, B.R., Flitter, W.D., Goldberg, D.E., Cerami, A., Henderson, G.B., *Proc. Natl. Acad. Sci. U. S. A.* **1991**, 88 (2), 325.

55. Bohle, D.S., Debrunner, P., Jordan, P.A., Madsen, S.K., Schulz, C.E., *J. Am. Chem. Soc.* **1998**, 120 (32), 8255.

56. Bohle, D.S., Dinnebier, R.E., Madsen, S.K., Stephens, P.W., *J. Biol. Chem.* **1997**, 272, 713.

57. Slater, A. F. G., Cerami, A., *Nature* **1992**, 355, 167.

58. Dorn, A., Stoffel, R., Matile, H., Bubendorf, A., Ridley, R.G., *Nature* **1995**, 374 (6519), 269.

59. Bendrat, K., Berger, B.J., Cerami, A., *Nature* **1995**, 378 (6553), 138.

60. Goldberg, D.E., Slater, A.F., Cerami, A., Henderson, G.B., *Proc. Natl. Acad. Sci.* **1990**, 87 (8), 2931.

61. Solomonov, I., Osipova, M., Feldman, Y., Baehtz, C., Kjaer, K., Robinson, I.K., Webster, G.T., McNaughton, D., Wood, B.R., Weissbuch, E., Leiserowitz, L., *J. Am. Chem. Soc.* **2007**, 129, (9), 2615.

62. Trager, W., *Trends Parasitol.* **2003**, 19 (9), 388.

63. Dorn, A., Vippagunta, S.R., Matile, H., Bubendorf, A., Vennerstron, J.L., Ridley, R. G., *Biochem. Pharmacol.* **1998**, 55 (6), 737.

64. Egan, T.J., Mavuso, W. W., Ncokazi, K. K., *Biochemistry* **2001**, 40 (1), 204. Epub 2001/01/05.

65. Egan, T. F., Tshivhase, M. G., *Dalton Trans.* **2006** 42, 5024.

66. Stiebler, R., Hoang, A. N., Egan, T. J., Wright, D. W., Oliveira, M. F., *PLoS One* **2010**, 5 (9), e12694.

67. Blauer, G., Akkawi, M., *Arch. Biochem. Biophys.* **2002**, 398 (1), 7.

68. Huy, N. T., Maeda, A., Uyen, D. T., Trang, D. T. X., Sasai, M., Shiono, T., Oida, T., Harada, S., Kamei, K., *Acta Trop.* **2007**, 101 (2), 130.

69. Jackson, K. E., Klonis, N., Ferguson, D. J. P., Adisa, A., Dogovski, C., Tilley, L., *Mol. Microbiol.* **2004**, 54 (1), 109.

70. Pisciotta, J., Coppens, I., Tripathi, A., Scholl, P., Shuman, J., Bajad, S., Shulaev, V., Sullivan Jr, D. J., *Biochem. J.* **2007**, 402 (Pt 1), 197.

71. Papalexis, V., Siomos, M. -A., Campanale, N., Guo, X. –G., Kocak, G., Foley, M., Tilley, L., *Mol. Biochem. Parasitol.* **2001**, 115 (1), 77.

72. Hoang, A. N., Sandlin, R. D., Omar, A., Egan, T. J., Wright, D. W., *Biochemistry* **2010**, 49 (47), 10107.

73. Hoang, A. N., Ncokazi, K. K., de Villiers, K. A., Wright, D. W., Egan, T. J., *Dalton Trans.* **2010**, 39 (5), 1235.

74. Egan, T. J., Combrinck, J. M., Egan, J., Hearne, G. R., Marques, H. M., Ntenteni, S., Sewell, B. T., Smith, P. J., Taylor, D., van Schalkwyk, D. A., Walden, J. C., *Biochem J.* **2002**, 365 (Pt 2), 343.

75. Egan, T. J., Chen, J. Y. –J., de Villiers, K. A., Mabotha, T. E., Naidoo, K. J., Ncokazi, K. K., *et al*. *FEBS Lett.* **2006**, 580, 5105.

76. Downie, M. J., Kirk, K., Mamoun, C. B., *Eukaryot. Cell*. **2008**, 7 (8), 1231.

77. Ben Mamoun, C., Prigge, S. T., Vial, H., *Drug Dev. Res.* **2010**, 71 (1), 44.

78. Woodrow, C. J., Krishna, S., eds, 'Molecular Approaches to Malaria: Glycolysis in Asexual-Stage Parasites', 1st edition, American Society for Microbiology, Washington D.C., **2005**.

79. Sato, S., Clough, B., Coates, L., Wilson, R. J. M., *Protist* **2004**, 155 (1), 117.

80. Bergman, G. J., *Sci. Edu.* **1948**, 32 (2), 93.

81. Warhurst, D., Craig, J., Adagu, I., Meyer, D., Lee, S., *Malar. J.* **2003**, 2 (1), 26.

82. Krogstad, D., Gluzman, I., Kyle, D., Oduola, A., Martin, S., Milhous, W., Schlesinger, P. H., *Science* **1987**, 238 (4831), 1283.

83. Asher, C., de Villiers, K. A., Egan, T. J., *Inorg. Chem.* **2009**, 48 (16), 7994.

84. de Villiers, K. A., Kaschula, C. H., Egan, T. J., Marques, H. M., *J. Biol. Inorg. Chem.* **2007**, 12 (1), 101.

85. Krogstad, D. J., Schlesinger, P. H., *Biochem. Pharmacol.* **1986**, 35, 547.

86. Moreau, S., Perly, B., Biguet, J., *Biochimie* **1982**, 64 (11–12), 1015. Epub 1982/11/01.

87. O'Neill, P. M., Willock, D. J., Hawley, S. R., Bray, P. G., Storr, R. C., Ward, S. A., Park, B. K., *J. Med. Chem.* **1997**, 40 (4), 437.

88. Cohen, S. N., Phifer, K. O., Yielding, K. L., *Nature* **1964**, 202, 805.

89. Chou, A. D., Chevli, R., Fitch, C. D., *Biochemistry* **1980**, 19 (8), 1543.

90. Egan, T. J., Ncokazia, K. K., *J. Inorg. Biochem.* **2004**, 98 (1), 144.

91. Egan, T. J., Mavuso, W. W., Ross, D. C., Marques, H. M., *J. Inorg. Biochem.* **1997**, 68 (2), 137.

92. Egan, T. J., *J. Inorg. Biochem.* **2006**, 100 (5–6), 916.

93. Buller, R., Peterson, M. L., Almarsson, O., Leiserwitz, L., *Cryst. Growth Des.* **2002**, 2 (6), 553.

94. Sullivan, D. J., Gluzman, I. Y., Russell, D. G., Goldberg, D. E., *Proc. Natl. Acad. Sci. U. S. A.* **1996**, 93 (21), 11865.

95. Dorn, A., Vippagunta, S. R., Matile, H., Jaquet, C., Vennerstrom, J. L., Ridley, R. G., *Biochem. Pharmacol.* **1998**, 55 (6), 727. Epub 1998/05/20.

96. de Villiers, K. A., Marques, H. M., Egan, T. J., *J. Inorg. Biochem.* **2008**, 102 (8), 1660.

97. Ignatushchenko, M. A., Winter, R. W., Riscoe, M., *Am. J. Trop. Med. Hyg.* **2000**, 62 (1), 77.

98. Winter, R. W., Cornell, K. A., Johnson, L. L., Ignatushchenko, M., Hinrichs, D. J., Riscoe, M. K., *Antimicrob. Agents Chemother.* **1996**, 40 (6), 1408.

99. Ignatushchenko, M. V., Winter, R. W., Bachinger, H. P., Hinrichs, D. J., Riscoe, M. K., *FEBS Lett.* **1997**, 409 (1), 67.

100. Kelly, J. X., Winter, R., Riscoe, M., Peyton, D. H., *J. Inorg. Biochem.* **2001**, 86 (2 -3), 617.

101. Kelly, J. X., Winter, R., Peyton, D. H., Hinrichs, D. J., Riscoe, M., *Antimicrob. Agents Chemother.* **2002**, 46 (1), 144.

102. Group, C. C. R., *J. Tradit. Chin. Med.* **1982**, 2, 3.

103. Meshnick, S. R., Taylor, T. E., Kamchonwongpaisan, S., *Microbiol. Rev.* **1996**, 60, 301.

104. Posner, G. H., Oh, C. H., Wang, D., Gerena, L., Milhous, W. K., Meshnick, S. R., Asawamahasadka, W., *J. Med. Chem.*, **1994**, 37, 1256.

105. Kamchonwongpaisan, S., Meshnick, S. R., *Gen. Pharmacol.* **1996**, 27, 587.

106. Meshnick, S., Yang, Y., Lima, V., Kuypers, F., Kamchonwongpaisan, S., Yuthavong, Y., *Antimicrob. Agents Chemother.* **1993**, 37 (5), 1108.

107. Zhang, F., Gosser Jr, D. K., Meshnick, R., *Biochem. Pharmacol.* **1992**, 43, 1805.

108. Bhisutthibhan, J., Pan, X. Q., Hossler, P. A., Walker, D. J., Yowell, C. A., Carlton, J., Dame, J. B., Meshnick, S. R., *J. Biol. Chem.* **1998**, 273, 16192.

109. Bhisutthibhan, J., Meshnick, S. R., *Antimicrob. Agents Chemother.* **2001**, 45, 2397.

110. Ellis, D. S., Li, Z. L., Gu, H. M., Peters, W., Robinson, B. L., Tovey, G., Warhurst, D. C., *Ann. Trop. Med. Parasitol.* **1985**, 79, 367.

111. Jiang, J. B., Jacobs, G., Liang, D. S., Aikawa, M., *Am. J. Trop. Med. Hyg.* **1985**, 34, 424.

112. Maeno, Y. T., Toyoshima, T., Fujioka, H., Ito, Y., Meshnick, S. R., Benakis, A., Milhous, W. K., Aikawa, M., *Am. J. Trop. Med. Hyg.* **1993**, 49, 485.

113. Johnson, J. D., Dennull, R. A., Gerena, L., Lopez-Sanchez, M., Roncal, N. E., Waters, N. C., *Antimicrobial. Agents Chemother.* **2007**, 51 (6), 1926.

114. Lucumi, E., Darling, C., Jo, H., Napper, A. D., Chandramohanadas, R., Fisher, N., Shone, A. E., Jing, J., Ward, S. A., Biagini, G. A., DeGrado, W. F., Diamond, S. L., Greenbaum, D. C., *Antimicrobial. Agents Chemother.* **2010**, 54 (9), 3597.

115. Baniecki, M. L., Wirth, D. F., Clardy, J., *Antimicrobial. Agents Chemother.* **2007**, 51 (2), 716.

116. Corbett, Y., Herrera, L., Gonzalez, J., Cubilla, L., Capson, T. L., Coley, P. D., Kursar, T. A., Romero, L. I., Ortega-Barria, E., *Am. J. Trop. Med. Hyg.* **2004**, 70, 119.

117. Rush, M. A., Baniecki, M. L., Mazitschek, R., Cortese, J. F., Wiegand, R., Clardy, J., Wirth, D. F., *Antimicrobial. Agents Chemother.* **2009**, 53 (6), 2564.

118. Kurosawa, Y., Dorn, A., Kitsuji-Shirane, M., Shimada, H., Satoh, T., Matile, H., Hofheinz, W., Masciadri, R., Kansy, M., Ridley, R. G., *Antimicrobial. Agents Chemother.* **2000**, 44 (10), 2638.

119. Koehn, F. E., Carter, G. T., *Nature Reviews Drug Discovery* **2005**, *4*, 206-220.

120. Bérdy, J., *J. Antibiot.* **2005**, *58*, 1-26.

121. Fenical, W., Jensen, P. R., Palladino, M. A., Lam, K. S., Lloyd, G. K., Potts, B. C., *Bioorganic and Medicinal Chemistry* **2009**, *17*, 2175-2180.

122. Carter, M., Phelan, V., Sandlin, R., Bachmann, B., Wright, D., *Combinatorial Chemistry & High Throughput Screening* **2010,** *13*, 285-292.

123. Mann, J., *Natural Product Reports* **2001,** *18*, 417-430.

124. Lam, K. S., *Current Opinion In Microbiology* **2006,** *9*, 245-251.

125. Chabala, J. C., Mrozik, H., Tolman, R. L., Eskola, P., Lusi, A., Peterson, L. H., Woods, M. F., Fisher, M. H., Campbell, W. C., *Journal of Medicinal Chemistry* **1980,** *23*, 1134-1136.

126. Fowler, A., Swift, D., Longman, E., Acornley, A., Hemsley, P., Murray, D., Unitt, J., Dale, I., Sullivan, E., Coldwell, M., *Analytical Chemistry* **2002,** *308*, 223-231.

127. Dixon, R.A, Ferreira, D., *Phytochemistry* **2002,** 60, 205-211.

128. Cunha-Rodrigues, M., Portugal, S., Prudencio, M., Goncalves, L. A., Casalou, C., Buger, D., Sauerwein, R., Haas, W., Mota, M. M., *PLoS ONE* **2008,** 3 (7), e2732.

129. Gazarini, M. L., Garcia, C. R. S., *Braz. J. Med. Biol. Res.* **2003,** 36, 1465-1469.